Geoscience Canada

Igneous Rock Associations 8. Arc Magmatism II:
Geochemical and Isotopic Characteristics

J. Brendan Murphy

Volume 34, Number 1, March 2007

URI: https://id.erudit.org/iderudit/geocan34_1ser01

See table of contents

Publisher(s)

The Geological Association of Canada

ISSN

0315-0941 (print)
1911-4850 (digital)

Explore this journal

Cite this article

Murphy, J. B. (2007). Igneous Rock Associations 8. Arc Magmatism II:: Geochemical and Isotopic Characteristics. *Geoscience Canada*, *34*(1), 7–35.

Article abstract

Geochemical and isotopic data provide insights into the origin and evolution of magmatism found at destructive plate margins. Tholeiitic magmas are dominant in the early stages of oceanic island-arc genesis and calc-alkalic magmas are most common in mature oceanic arcs and in continental arcs where they may range from basalt to rhyolite in composition, including voluminous intermediate (andesitic) rocks. Experiments suggest that calcalkalic mafic magmas are formed by melting of a hydrated mantle wedge and undergo low pressure fractional crystallization under near-H2O saturated conditions. Intermediate to felsic magmas are derived in a wide variety of ways, including the fractionation of a more mafic parent, mixing between mafic and felsic magmas (a process supported, in many cases, by field and textural evidence), crustal contamination, or partial melting of the crust. All these processes appear to take place, to some degree, in arc systems, although in any given arc system, one mechanism may predominate.

Arc-related calc-alkalic and tholeiitic basalts typically show moderate degrees of light rare-earth-element (LREE) enrichment, and flat heavy rare-earth-element (HREE) profiles, indicating an origin in a shallow (spinel lherzolite) mantle. More evolved magmas exhibit Eu anomalies, consistent with low pressure plagioclase fractionation. Compared to within-plate settings, tholeiitic and calc-alkalic arc magmas have lower abundances in high-field-strength (HFS) elements, possibly because these elements are bound during the accessory phases in the mantle wedge, and are stable during partial melting. Compared to arc tholeiites, calc-alkalic magmas have higher abundances of incompatible large ion lithophile (LIL) elements reflecting enrichment in the mantle wedge source. This characteristic depletion in HFS, and enrichment in LIL, elements, in arc magmas is the basis for a variety of discrimination diagrams. These diagrams constrain processes operating in modern and ancient arc systems and include chondrite-normalized, MORB-normalized and mantle-normalized spidergrams, which are characterized by jagged patterns of trace-element abundances (in contrast to the relatively smooth patterns of within-plate suites).

Some arc suites have depleted initial 143Nd/144Nd and lower initial 87Sr/86Sr than the bulk earth, and are similar to MORB. Other suites have enriched isotopic patterns consistent with the influence of subducted oceanic sediments on the composition of the magma. Samarium-Nd and Rb-Sr isotopic studies can be used to distinguish between felsic magmas derived from fractional crystallization of a more mafic parent (which would have similar values) and those derived from the melting of ancient crust.

SERIES

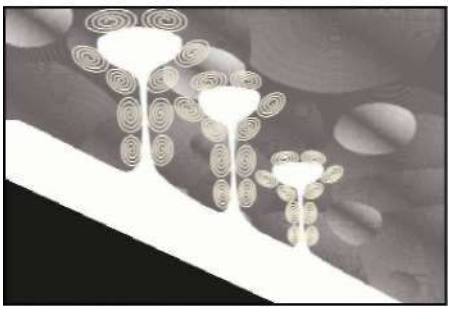

Igneous Rock Associations 8. Arc Magmatism II: Geochemical and Isotopic Characteristics

J. Brendan Murphy
Dept of Earth Sciences, St. Francis Xavier University, Antigonish, NS, B2G 2W5, Canada
E-mail: bmurphy@stfx.ca

SUMMARY

Geochemical and isotopic data provide insights into the origin and evolution of magmatism found at destructive plate margins. Tholeiitic magmas are dominant in the early stages of oceanic island-arc genesis and calc-alkalic magmas are most common in mature oceanic arcs and in continental arcs where they may range from basalt to rhyolite in composition, including voluminous intermediate (andesitic) rocks. Experiments suggest that calc-alkalic mafic magmas are formed by melting of a hydrated mantle wedge and undergo low pressure fractional crystallization under near-H_2O saturated conditions. Intermediate to felsic magmas are derived in a wide variety of ways, including the fractionation of a more mafic parent, mixing between mafic and felsic magmas (a process supported, in many cases, by field and textural evidence), crustal contamination, or partial melting of the crust. All these processes appear to take place, to some degree, in arc systems, although in any given arc system, one mechanism may predominate.

Arc-related calc-alkalic and tholeiitic basalts typically show moderate degrees of light rare-earth-element (LREE) enrichment, and flat heavy rare-earth-element (HREE) profiles, indicating an origin in a shallow (spinel lherzolite) mantle. More evolved magmas exhibit Eu anomalies, consistent with low pressure plagioclase fractionation. Compared to within-plate settings, tholeiitic and calc-alkalic arc magmas have lower abundances in high-field-strength (HFS) elements, possibly because these elements are bound during the accessory phases in the mantle wedge, and are stable during partial melting. Compared to arc tholeiites, calc-alkalic magmas have higher abundances of incompatible large ion lithophile (LIL) elements reflecting enrichment in the mantle wedge source. This characteristic depletion in HFS, and enrichment in LIL, elements, in arc magmas is the basis for a variety of discrimination diagrams. These diagrams constrain processes operating in modern and ancient arc systems and include chondrite-normalized, MORB-normalized and mantle-normalized spidergrams, which are characterized by jagged patterns of trace-element abundances (in contrast to the relatively smooth patterns of within-plate suites).

Some arc suites have depleted initial $^{143}Nd/^{144}Nd$ and lower initial $^{87}Sr/^{86}Sr$ than the bulk earth, and are similar to MORB. Other suites have enriched isotopic patterns consistent with the influence of subducted oceanic sediments on the composition of the magma. Samarium-Nd and Rb-Sr isotopic studies can be used to distinguish between felsic magmas derived from fractional crystallization of a more mafic parent (which would have similar values) and those derived from the melting of ancient crust.

SOMMAIRE

Les données géochimiques et isotopiques fournissent des indications quant à l'origine et à l'évolution du magmatisme des marges de subduction des plaques tectoniques. Les magmas sont principalement tholéiitiques dans les premières phases de formation des arcs insulaires océaniques, alors qu'ils sont principalement calco-alcalins pendant les phases terminales des arcs insulaires océaniques ainsi que dans les arcs insulaires continentaux, où leur composition peut aller du basalte à la rhyolite, dont des volumes considérables de roches de composition intermédiaire (andésitique). Des expériences permettent de penser que les magmas mafiques calco-alcalins sont formés par la fusion d'un biseau mantélique hydraté qui subit une cristallisation

fractionnée à basse pression en des conditions de quasi-saturation en H_2O. Les magmas de composition intermédiaire à felsique résultent de mécanismes très variés, dont le fractionnement d'une roche mère plus mafique, le mélange de magmas felsiques et mafiques (mécanismes mis en évidence par des données de terrain et l'analyse texturale), la contamination crustale, ou la fusion partielle de la croûte. Tous ces mécanismes semblent se produire, au moins partiellement, au sein d'arcs insulaires, mais l'un d'eux peut constituer le mécanisme prédominant de quelque système d'arcs insulaires particulier.

L'enrichissement modéré typique des basaltes calco-alcalins et tholéiitiques d'arcs insulaires en éléments légers des terres (LREE) rares ainsi que le profil plat de leur contenu en éléments lourds des terres rares (HREE) sont des indicateurs d'une origine mantélique peu profonde (iherzolithe à spinelle). Les magmas plus évolués affichent des anomalies en Eu, ce qui concorde avec un fractionnement à basse température des plagioclases. Comparés à ceux des contextes intra-plaques, les magmas tholéiitiques et calco-alcalins d'arcs insulaires affichent des contenus moindres en éléments à grande intensité de champ, peut-être parce que ces éléments sont liés pendant les phases accessoires dans le biseau mantélique, et sont stables pendant la phase de fusion partielle. Comparés aux tholéiites d'arcs insulaires, les magmas calco-alcalins ont des contenus plus élevés en éléments lithophiles à grands champs ioniques incompatibles, ce qui est le reflet d'un enrichissement au sein du biseau mantélique source. Cet appauvrissement caractéristique en éléments à grande intensité de champ (HFS) et cet enrichissement en éléments lithophiles à grands champs ioniques (LIL) des magmas d'arcs insulaires forment la base d'une variété de diagrammes de discrimination. Ces diagrammes permettent de préciser les processus en jeu des systèmes d'arcs insulaires modernes et anciens et incluent des diagrammes radiaux normalisés pour les chondrites, pour les basaltes de dorsales océaniques (MORB) et pour le manteau, lesquels son caractérisés par des profils anguleux irréguliers des courbes de contenus en éléments traces (en contraste avec les profils relativement réguliers des suites intra-cratoniques).

Certaines suites d'arcs insulaires montrent des ratios initiaux $^{143}Nd/^{144}Nd$ appauvris et $^{87}Sr/^{86}Sr$ inférieurs à celui de la valeur planétaire actuelle, et qui sont semblables à celui des basaltes de dorsales océaniques. D'autres suites ont des profils isotopiques enrichis, ce qui correspond à une influence de sédiments océaniques subductés sur la composition du magma. Les études samarium-néodymium et rubidium-strontium peuvent être utilisées pour différencier entre les magmas felsiques issus d'une cristallisation fractionnée d'une roche mère plus mafique (qui montrerait des valeurs similaires) et ceux provenant de la fusion d'une croûte ancienne.

INTRODUCTION

This is the second of two articles on arc magmatism intended for geoscientists who do not specialize in petrology or geochemistry. The first article (Murphy 2006) explored the broad relationship between the tectonic evolution of arcs and magma genesis, composition and evolution. This article focuses on the geochemical, isotopic and petrological evolution of arc magmas. For a more detailed analysis, the reader is referred to comprehensive reviews of the geochemical and petrological aspects of arc magmatism in papers (e.g. Arculus and Curran 1972; Ringwood 1977; Pearce and Norry 1979; Gill 1981; Pearce 1982; Tatsumi and Eggins 1995; Morris and Ryan 2004; Keleman 2004) and in recent textbooks (e.g. Winter 2001; Blatt et al. 2005).

Arc magmatism is the end result of subduction of oceanic lithosphere caused by the sinking of a dense oceanic plate beneath an adjacent, less dense overriding plate (Fig. 1). This descent is characterized by a long, narrow, curvilinear trench in the ocean floor. With rare exceptions, magmas form in the mantle wedge above the subduction zone (i.e. in the overriding plate), and/or the crust. These magmas ascend to form arcs, either continental arcs (e.g. the Andes) or island arcs (e.g. the western Pacific Ocean). Island arcs capped by oceanic crust are dominated by mafic magmatism, and those capped by continental crust by felsic magmatism. Magmatism is also important in the “backarc” region behind these arcs, especially during episodes of extension.

This article begins with an overview of the major-, trace- and rare-earth chemistry of arc magmas to provide constraints on the source of the magmas and their subsequent evolution. This is followed by a review of the principles behind tectonic and magmatic discrimination diagrams including the so-called “spider diagrams” and the information they provide about petrogenesis. A review of petrogenetic-indicating isotopes is presented, which helps constrain the source regions of magmas and the relationships among coeval mafic, intermediate and felsic magmas. Some of the less common igneous rocks that can occur in arc settings (e.g. adakites, shoshonites, and boninites) are reviewed and the paper concludes with a brief overview of arc rocks in ancient settings.

MAGMA CHEMISTRY

In contrast to most other tectonic regimes, arc plutonic and volcanic rocks are characterized by chemical diversity as shown by their wide distribution on standard classification schemes (e.g. Streckeisen 1976, 1979; LeMaitre et al. 1989), and range from mafic to felsic in composition. There are, however, some useful generalities. Mafic rocks, such as gabbros and basalts, tend to be most abundant in

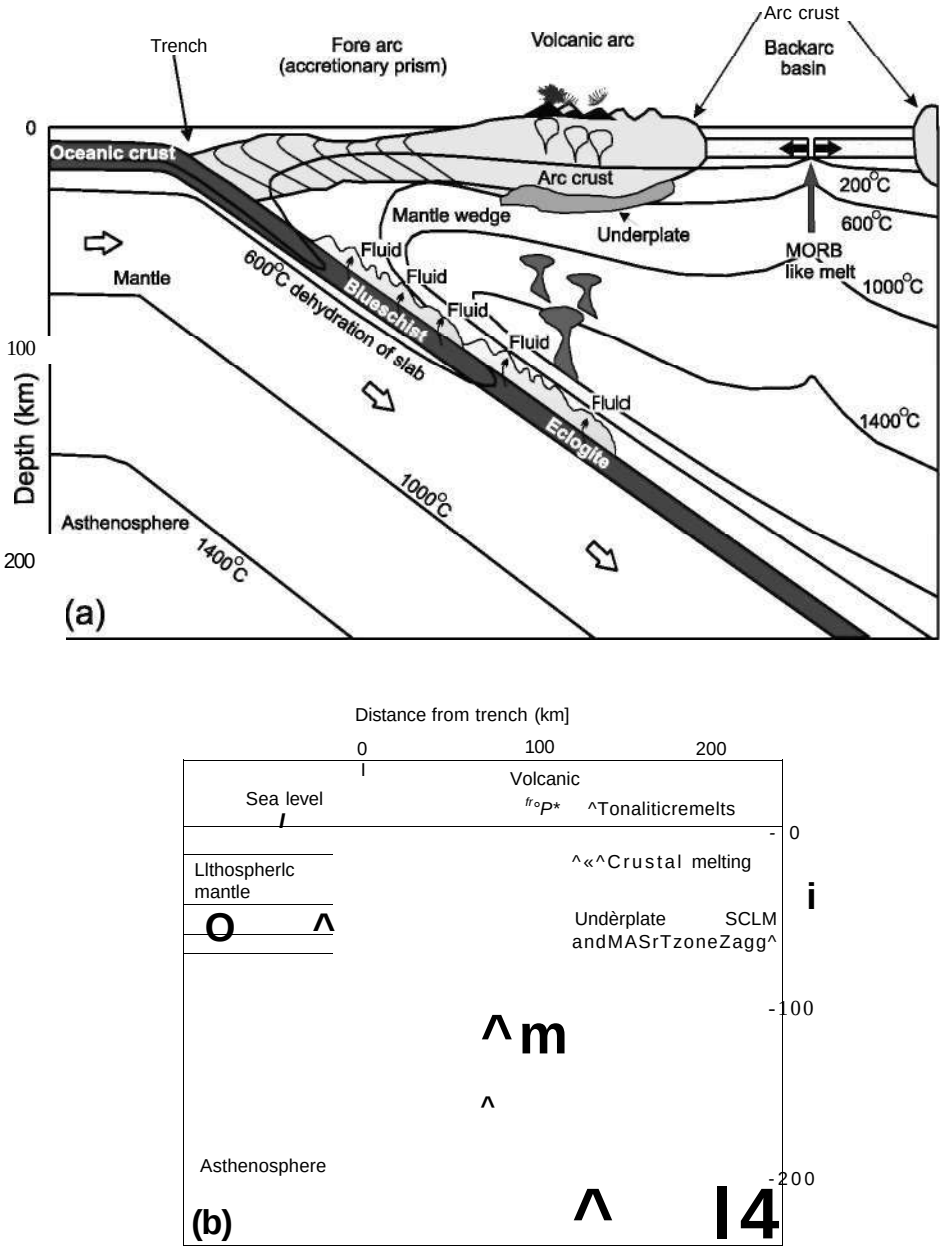

Figure 1. Diagrams showing how (a) island arcs, and (b) continental arcs are formed (modified after Winter, 2001). Dehydration reactions form blueschist and eclogite at depth in the vicinity of the subducted oceanic slab. Water released from dehydration invades the overlying mantle wedge causing melting in the mantle. Rising mafic magmas may underplate the crust. (a) Subduction of denser (and older) oceanic lithosphere beneath less dense lithosphere to create an island arc. The less dense lithosphere may consist of younger oceanic lithosphere capped by oceanic crust (e.g. Marianas) or a microcontinent (e.g. Japan). Roll-back of the subduction zone (see Dewey 1980; Collins 2002) may create a backarc basin. (b) Subduction of oceanic lithosphere beneath a continental margin (e.g. Andes) to form a continental arc. Note that in both cases, the direction of subduction (given by arrows) is oblique to the subduction zone. MORB: Mid-Ocean Ridge Basalts; SCLM: Sub-Continental Lithospheric Mantle; MASH: Mixing-Assimilation-Storage-Homogenization.

primitive oceanic arcs. With increasing arc maturity, and/or crustal thickness, intermediate to felsic magmas (diorites to granites, andesites to rhyolites) predominate (e.g. Miyashiro 1974). Except for some special cases, even the most mafic arc rocks are quartz-normative. Alkali-rich rocks and feldspathoidal rocks are rare (feldspathoids and quartz are mutually exclusive) and plagioclase typically dominates over alkali-feldspar.

In recent years, chemical studies of arc magmas have integrated data from major elements (those that typically comprise 0.1 wt % or higher), trace elements (less than 0.1 wt %), rare-earth elements (generally the "lanthanides") and isotopes (typically Rb-Sr, Sm-Nd and U-Pb systems). Important goals of these studies are to determine i) the nature of the source region of arc magmas, ii) how the magma chemistry evolves as it rises toward the surface and interacts with its surroundings, and iii) the cooling history as the magma is transformed into igneous rock.

Phase equilibria predict that intermediate and felsic rocks can originate by fractional crystallization of a more basic parent because the early fractionation of olivine, clinopyroxene and plagioclase drives the liquid toward more silicic compositions (Fig. 2). Experimental and theoretical studies (e.g. Grove and Baker 1984; Ghiorso and Sack 1995) show that this fractionation scheme yields a tholeiitic trend (i.e. significant enrichment in FeO*/MgO) because the fractionating phases contain lower FeO*/MgO than the melt (note that FeO* is the symbol for total iron oxide, in which FeO and Fe_2O_3 are combined). However, in the simplest sense, this process should produce volumetrically less andesite than basalt, and still less rhyolite. So, many authors consider it unlikely that such a process could, by itself, yield the vast volumes of andesitic and rhyolitic magmas that occur in mature arcs, even if magnetite were to appear on

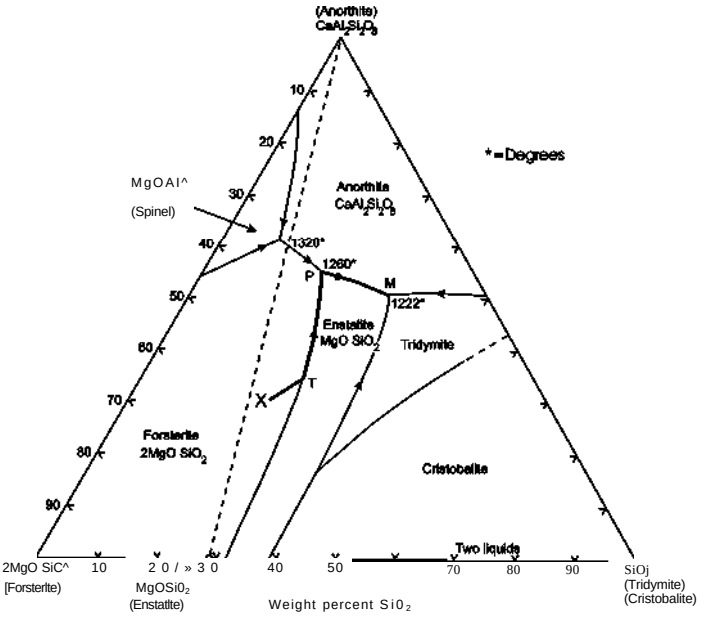

Figure 2. Phase diagram showing the cooling path of mafic magma (heavy line) of bulk composition X. Olivine crystallizes first (X-T), followed by pyroxene (T-P) and plagioclase (P-M). When the olivine is expired (at P under equilibrium conditions), the liquid path migrates down temperature to M where tridymite (which forms quartz when cooled) begins to crystallize. Note that partial melting of any source rock in the Anorthite-Enstatite-Quartz triangle would initially yield a melt of composition M, whereas partial melting of any source rock in the Fosterite-Enstatite-Anorthite triangle would initially yield a melt of composition P. Thus partial melting yields magmas of the same composition over a wide range of bulk compositions.

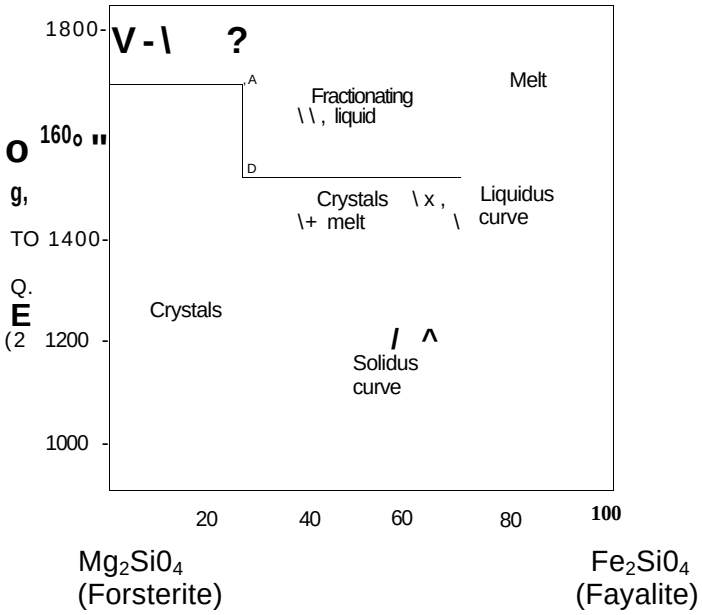

Figure 3. Binary phase diagram showing how the Fe/Mg ratio in olivine increases during cooling. Bulk composition (X) at 1800°C cools to 1700°C at which point forsterite crystals (point B) coexist with the melt (point A). With cooling, the liquid and crystals both become richer in Fe/Mg. Under equilibrium crystallization conditions, all liquid will have expired when the crystals attain an Fe/Mg ratio equal to that of the starting liquid (point D). Under fractional crystallization conditions, the liquids and crystals continue to evolve towards more Fe/Mg rich compositions, depending on the extent of crystal fractionation.

the liquidus to subdue iron enrichment trends.

Alternatively, ongoing underplating by mantle-derived magma delivers a significant amount of heat to the base of the crust, eventually sufficient to induce partial melting of crust, which typically produces felsic magmas (see Murphy 2006, fig.16). Many arc systems, especially those capped by thick continental crust, have mafic magmas derived from the mantle, intermediate to felsic magmas formed by fractionation of a more mafic parent, and felsic magmas that are derived by partial melting of the crust. Magmas with intermediate compositions can also be produced by mixing at depth of mafic and felsic end-member compositions (e.g. Eichelberger 1975; Gill 1981; Carmichael 2002). There is a general consensus that all these processes occur to some degree in arc systems, and in any locality, it can be challenging to distinguish among them.

Major Element Chemistry

Major element abundances profoundly influence physical properties such as magma viscosity and density, which in turn affect the rate at which magmas rise in the crust. The major element chemistry of parental magmas formed by partial melting is primarily controlled by phase equilibria. This principle is shown schematically in Figure 2 in which a magma of composition M, representing the minimum temperature in the system, is produced by melting of host rocks (e.g. X) with a wide range of bulk compositions. Once magma is produced, its major-element composition mostly controls what silicate minerals eventually grow from the magma, and so the chemical evolution of the cooling magma is constrained by phase equilibria. Experimental and observational evidence suggest that olivine, followed by clinopyroxene and plagioclase, are the earliest crystallizing phases from mafic magma. Fractional crystallization of ferromagnesian phases such as olivine and clinopyroxene leads to systematic depletion in FeO*, MgO, and enrichment in elements such as SiO_2, Na_2O and K_2O. When plagioclase appears on the liquidus, the remaining liquid becomes depleted in CaO and Al_2O_3. Figure 2 shows the evolution of a typical basaltic liquid in

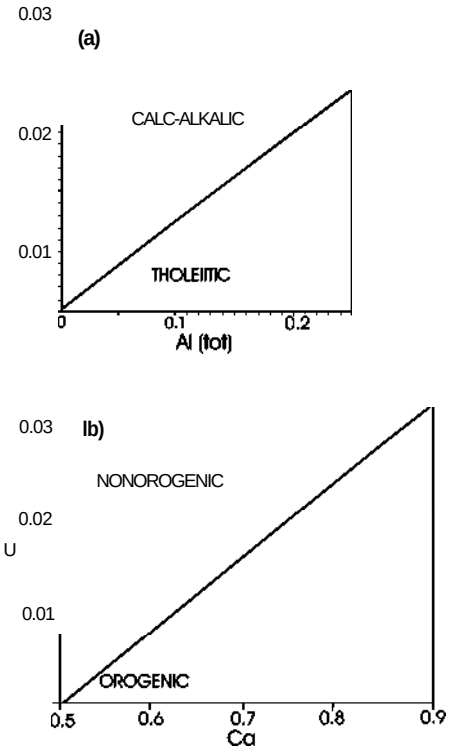

Figure 4. Bivariate diagrams (Letterier et al. 1982) showing how the chemical composition of clinopyroxene reflects the (a) calc-alkalic vs tholeiitic, and (b) orogenic vs non-orogenic conditions in which it formed.

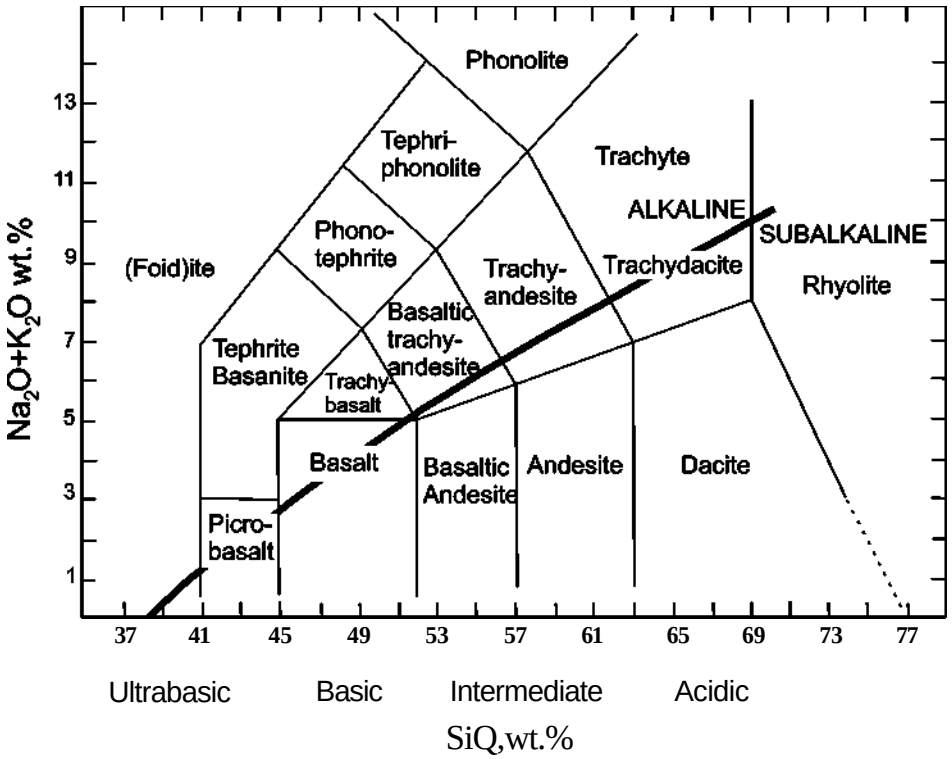

Figure 5. SiO_2 vs Na_2O + K_2O diagram (see Irvine and Baragar 1971; Cox et al. 1979 and LeMaitre et al. 1989) which classifies rock types and discriminates between alkalic and subalkalic rocks.

a shallow magma chamber (i.e. low pressures). As long as the system remains closed, cooling of a basaltic liquid of composition X will initially produce forsterite (olivine), and then enstatite. Equilibrium crystallization or fractionation of these minerals drives the residual liquid composition away initially from olivine (X to T) until it reaches and then descends the olivine-enstatite curve (T to P). Along pathway X to P, the magma becomes enriched in other components, including those of plagioclase (represented by anorthite). As path T to P is along a reaction curve, olivine reacts with the liquid and enstatite is precipitated. Once plagioclase begins to crystallize, the residual magma also becomes depleted in CaO and Al_2O_3. The overall result is that mafic liquids evolve towards more intermediate and felsic compositions.

The composition of the minerals also reflects fractionation. The FeO*/MgO ratio found in the olivines and pyroxenes increases with fractionation, as shown, for example, in the simple phase relationships in Figure 3. Olivine and clinopyroxene phenocrysts in arc basalts are more iron-rich than those that are in equilibrium with mantle rocks, suggesting that even the most primitive arc magmas are fractionated to some degree and that true primary magmas (i.e. melts directly derived from the mantle) are rare.

Mineral compositions are also susceptible to the tectonic environment in which they are formed. For example, Leterrier et al. (1982) showed that for clinopyroxenes of similar Ca content, those in arc-related mafic rocks have lower Ti + Cr than those in non-orogenic settings (Fig. 4).

As most volcanic rocks are dominated by a glassy or fine grained matrix, their minerals are poorly developed and so they are more effectively classified by their chemistry rather than their mineral content. The most familiar classification of lavas is based on silica content (Fig. 5). However, arc magmas are so chemically diverse, that to be able to understand the petrologic processes responsible, additional elements must be used. Magmas with similar silica content can be distinguished from one another by examining the concentration of other elements. For example, many basalts in subduction zone environments are characterized by high Al_2O_3 (17.0 – 21.0 wt %) and low MgO (< 6 wt %), compared with basalts in other tectonic settings, and are known as *high-alumina basalt*. Although their origin is unclear, their low MgO content suggests that they are fractionated (by removal of olivine and augite) from a more mafic parent. The high Al_2O_3 implies that plagioclase was not a liquidus phase.

Two suites, or collections of magmas, known as *alkalic* and *subalkalic*, can be distinguished on the basis of their alkali content (Na_2O + K_2O; MacDonald 1968; Cox et al.

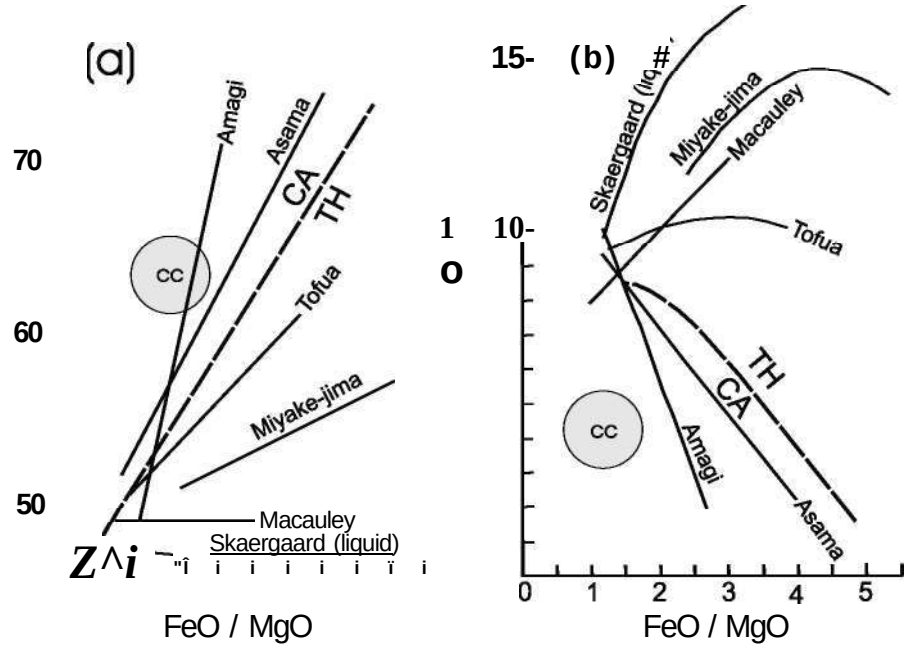

Figure 6. (a) FeOt/MgO vs SiO_2, and (b) FeOt/MgO vs FeOt plots for subalkalic rocks (after Miyashiro 1974). FeOt = total iron oxide. Note that the dashed line dividing calc-alkalic (CA) and tholeiitic (TH) suites is not a discriminant line; rather it is a reference slope. Suites that have trends steeper than the discriminant slope (i.e. relatively steep rise in FeO*/MgO and FeOt) are classified as tholeiitic, whereas suites with shallower trends (a more subdued rise in FeO*/MgO and FeOt) are classified as calc-alkalic. cc = continental crust.

1979; Wilson 1989; Rollinson 1993). For the same silica content, alkalic basalts have higher $Na_2O + K_2O$ than subalkalic basalts, and alkalic rhyolites have higher $Na_2O + K_2O$ than subalkalic rhyolites (Fig. 5). Subalkalic suites are further divided into *tholeiitic* or *calc-alkalic* suites on the basis of their FeO* and MgO contents. In both suites, FeO* and MgO decreases with fractionation, which suggests the importance of ferromagnesian minerals, such as olivine and pyroxene in the evolution of both types of magma. However, for rocks of the same silica content, tholeiitic rocks have higher FeO*/MgO ratios than calc-alkalic rocks (Miyashiro 1974; Fig. 6).

Even within an individual suite, there are further distinctions that can be made. For example, tholeiitic rocks that occur in arc environments can be distinguished from tholeiitic rocks in other settings by the concentrations of other elements, including their K_2O content, which tends to be lower than in rift-related tholeiites (e.g. Gill 1981). These *island-arc tholeiites* (IAT) are also known as "low-K tholeiites" and typically have $K_2O < 0.8$ wt%.

Although the generation of each suite of rocks is controversial, there are some general over-arching principles. Using the Japanese arc as an example, Kuno (1966) drew attention to the increasing K_2O content in rocks that have similar SiO_2, with increasing distance from the trench (and hence greater height above the subduction zone), the so-called *K-h* relationship (Dickinson 1975). Thus tholeiitic basalts, which typically occur nearer to the trench, have lower K_2O contents than calc-alkalic basalts, whose K_2O content increases farther away from the trench. Gill (1981) recognized volumetrically small, but petrologically significant, potassic-rich basaltic to intermediate lavas, known as *shoshonites* that occur far from the trench in continental arcs.

Some experimental data suggest that high P_{CO2} in the mantle may yield silica-undersaturated (i.e. olivine-nepheline normative) alkalic basalts whereas high P_{H2O} produces silica-saturated basalts (e.g. Mysen and Boettcher 1975, Boettcher 1977; Eggler 1978; Mysen 1988). As alkalies readily partition into melt, alkalic basalts are thought to represent small degrees of partial melting, possibly from a source mantle previously enriched in alkalies. However, the ascent of such small volumes of melt is mechanically problematic (see Murphy 2006) and so alkalic magmas in arc settings tend to be restricted to specialized settings, such as local rift zones within the arc or backarc region.

The major element composition of calc-alkalic and tholeiitic lavas is reflected in their mineral contents. Arc lavas, especially calc-alkalic lavas, contain abundant phenocrysts and microphenocrysts (up to 20%). A summary of the range of phenocryst content with magma type and composition is shown in (Table 1; after Wilson 1989). Plagioclase is the most abundant phenocryst, and occurs in both calc-alkalic and tholeiitic suites in lavas that range from basaltic to rhyolitic in composition. Plagioclase is characterized by complex zoning patterns that reflect disequilibrium conditions (Shelley 1993; Stewart and Fowler 2001; Murphy 2006) For both tholeiitic and calc-alkalic suites, clinopyroxene phenocrysts occur in mafic to intermediate lavas, olivine phenocrysts are typically restricted to the more mafic lavas and orthopyroxene, amphibole and quartz phenocrysts are more common in intermediate to felsic lavas. Many phenocrysts, like plagioclase, exhibit textural and chemical evidence of disequilibrium. Although magnetite is a common phenocryst in intermediate to felsic lavas of both magma series, it also occurs as a phenocryst in mafic lavas

Table 1. Typical phenocryst content of island arc tholeiitic and calc-alkalic basalt (B), basaltic andesite (BA), andesite (A), dacite (D) and rhyolite (R) (after Wilson 1989). Solid lines, common; dashed lines, rare.

	B	BA	A	D	R
low-K tholeiite					
olivine					
clinopyroxene					
plgeonlte					
orthopyroxene					
amphibole					
biotite					
magnetite					
plagioclase					
alkali feldspar					
quartz					
medium-K calc alkaline					
olivine					
clinopyroxene					
plgeonlte					
orthopyroxene					
amphibole					
biotite					
magnetite					
plagioclase					
alkali feldspar					
quartz					
high-K calc alkaline					
olivine					
clinopyroxene					
plgeonlte					
orthopyroxene					
amphibole					
biotite					
magnetite					
plagioclase					
alkali feldspar					
quartz					

in calc-alkalic suites.

As the calc-alkalic suite is the most dominant suite in arc environments, especially so in mature arcs, the processes responsible for their limited increase in FeO*/MgO have received considerable attention. Phase-equilibria studies show that, like tholeiites, fractionation of olivine and pyroxene are important in the earliest stages of fractionation of calc-alkalic magmas. Miyashiro (1974) proposed that water derived from the subduction zone leads to oxidized melts, and the early precipitation of oxide minerals such as magnetite (Fe_3O_4). This interpretation is consistent with petrographic observations that magnetite is a common phenocryst in basaltic calc-alkalic basalts but is rare in tholeiitic basalts. Precipitation of magnetite would inhibit enrichment in FeO*/MgO with fractionation, leading to a calc-alkalic trend. Experimental evidence, however, yields conflicting results. Lee et al. (2005) found that the oxidation state of the magma in arc environments is similar to that of the mid-ocean ridge basalts (MORB), and that the degree of oxidation might be buffered by mantle mineral assemblages. Sisson and Grove (1993) show that low pressure (2 kb) fractionation of a H_2O-rich (4-6 wt %) basalt can reproduce calc-alkalic trends by crystallization of olivine, Ca-rich plagioclase (An > 90) and either magnetite or spinel. Ringwood (1977) and Boettcher (1977) point out that H_2O-rich magmas would increase the stability of hornblende, which would have a similar FeO*/MgO to the melt. Fractionation of hornblende would also inhibit the increase of FeO*/MgO during fractionation and so produce a calc-alkalic trend. The importance of amphibole as a phenocryst in intermediate rocks suggests it may play a role at this stage in the cooling of the magma.

Although there are some controversies, it is generally accepted that water plays a major role in producing calc-alkalic magmas, and so it is not surprising that these magmas are the dominant suite in many arcs. Several experimental studies (e.g. Sisson and Grove 1993; Grove et al. 2003) suggest that calc-alkalic magmas form by hydrous melting of the mantle, and then rise to the shallow crust where they undergo fractional crystallization under near-H_2O saturated conditions. Sisson et al. (2005) point out that a significant quantity of rhyolitic liquid can be derived by differentiation or by low-degree partial re-melting of mantle-derived basalt.

Another alternative is that calc-alkaline trends and high volume of intermediate magmas are generated by mixing of mafic and felsic end-member magmas. This is supported by widespread petrographic evidence of textural disequilibrium in andesites (e.g. Eichelberger 1975; Eichelberger et al. 2000, 2006), and by geochemical and isotopic patterns consistent with mixing (Grove et al. 2005; see also the discussion below) and field observations (e.g. Wiebe et al. 2002).

Although several exceptions have been documented, arc magmas exhibit broad chemical trends in space and time during arc evolution. Tholeiitic magmas are common in the early stages of oceanic island-arc genesis and are closer to the trench. The calc-alkalic suite of magmas is the most common in mature oceanic arcs and generally occurs farther from the trench than arc tholeiites; this suite is especially common in continental arcs. There is also a tendency in both suites toward more silicic compositions with increasing arc maturity and crustal thickness,

Table 2. Partition coefficients for various trace elements in rock-forming minerals (see Winter 2001, p. 157; Pearce and Norry 1979).

	cpx	opx	plag	olivine	garnet	spinel	ilmenite	magnetite	apatite	amph
Ni	7.0	5.0	0.01	14.0	0.955			29		6.8
Cr	34.0	10.0	0.01	0.70	1.345			7.4		2.00
Rb	0.004	0.005	0.08	0.00001	0.00001	0.32	0.001	0.32		0.29
Ba	0.002	0.0006	0.16	0.00001	0.00001	0.001	0.01	0.001		0.42
Nb	0.006	0.004	0.0236	0.00353	0.01	0.08	2.3	0.1		0.8
La	0.05	0.016	0.042	0.000007	0.001	0.0006	0.0072	0.029	3.4	0.544
Ce	0.08	0.04	0.036	0.00001	0.005	0.0006	0.00783	0.0217	4.5	0.843
Sr	0.079	0.062	1.97	0.00012	0.0005	0.4	0.7	0.4	3.7	0.46
Nd	0.18	0.037	0.029	0.00007	0.04	0.0006	0.00847	0.0145	6.7	1.804
Zr	0.13	0.03	0.09	0.003	0.9	0.04	0.33	0.1	0.9	0.5
Sm	0.29	0.054	0.022	0.0007	0.21	0.0006	0.0091	0.0072	6.7	1.340
Eu	0.33	0.063	0.22	0.00095	1	0.0006	0.0084	0.00635	6.7	1.557
Ti	0.36	0.08	0.045	0.017	0.28	0.07	16	7.5		1.5
Y	0.41	0.3	0.01	0.0074	3.1	0.0039	0.0045	0.0039		1.0
Dy	0.46	0.1621	0.013	0.004	3.8	0.0015	0.0106	0.0071	5.1	
Er	0.38	0.1816	0.013	0.009	4.5	0.003	0.01625	0.0117	4.0	1.740
Yb	0.42	0.2605	0.012	0.023	5.5	0.0045	0.02475	0.01923	2.9	1.642
Lu	0.45	0.318	0.012	0.03	7.1	0.0045	0.029	0.023	2.3	1.563

and many calc-alkalic suites range from basaltic to rhyolitic composition, and are typified by an abundance of intermediate (andesitic) rocks.

Trace Element and REE Geochemistry

Trace element, rare-earth-element (REE) and isotopic abundances reflect a variety of factors including the source of the magma, the percentage of the source rock that undergoes melting, the extent of crystal fractionation, and the contamination of either magma from adjacent rocks or from other magmas of other arc systems. In each case, trace element abundances can be modelled (see Appendix 1).

Trace element and REE abundances are sensitive to the appearance of minerals as liquidus phases. For example, Ni and Cr are heavily concentrated into early-crystallizing minerals such as olivine and pyroxene, and Y, Yb and Lu are concentrated in garnet. The fractionation of olivine and pyroxene depletes the remaining liquid in Ni and Cr, providing a sensitive indicator on the extent of their fractionation. Such elements are also known as *compatible* trace elements because they fit into the structure of early crystallizing minerals and so have a low concentration in the melt. Alternatively, trace elements such as Zr, Hf, Nb, Ta, Ti, and Th are known as *incompatible* trace elements. They strongly partition into magma, and so their abundances should increase systematically during crystal fractionation. Note that some elements behave incompatibly in some magmas but compatibly in others. For example, Ti is concentrated in hornblende and both V and Ti are concentrated in magnetite. Nevertheless, these minerals can crystallize early or late in the evolution of magmas depending on P_{H2O} and fO_2 (e.g. Miyashiro 1974; Ringwood 1977). Most calc-alkalic suites record a decrease in Ni, Cr, Ti and V from basalt to andesite, consistent with experimental evidence for the fractionation of olivine and magnetite.

Generally, early crystallizing minerals such as olivine, clinopyroxene, plagioclase and orthopyroxene contain very low REE abundances (Table 2). Therefore, the REE are incompatible elements and partition into the melt causing the total REE to increase during fractionation from mafic to intermediate magmas. As the magma cools, REE elements eventually become concentrated in accessory phases such as zircon, rutile, ilmenite, titanite and monazite. In some highly siliceous magma, precipitation of accessory minerals is common (Miller and Mittlefehldt 1982) so that REE abundances can decrease during the later stages of magma evolution. Rare-earth-element abundances are most commonly displayed on diagrams in which the lanthanide elements are arranged from left to right with increasing atomic number (57-71, La to Lu on the periodic table). The lanthanides have similar chemical and physical properties (all but Eu are trivalent) and their ionic radius decreases with increasing atomic number (the so-called "lanthanide contraction"); Europium can be divalent or trivalent depending on the degree of oxidation of the magma. According to Goldschmidt's rules, if ions have the same charge, the smaller ions are preferentially incorporated into growing crystals.

The concentration of each

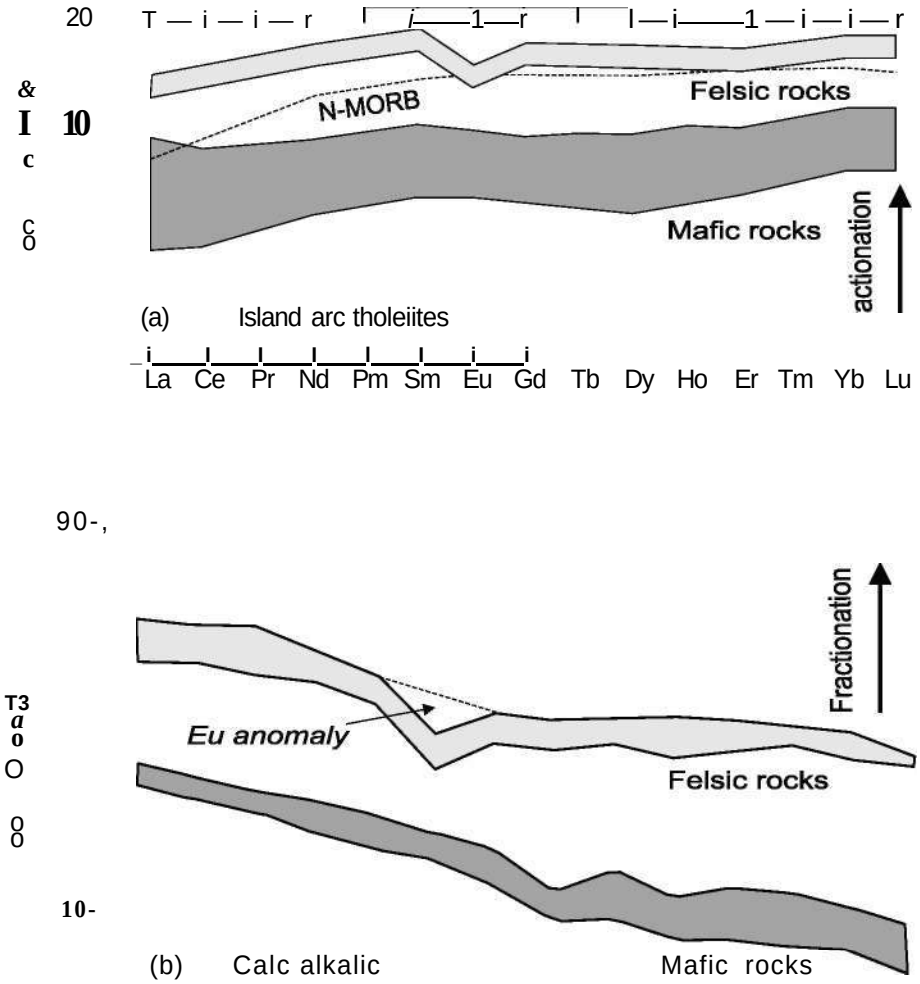

Figure 7. Typical chondrite-normalized rare-earth-element (REE) plots (after Sun and McDonough 1989; see also Greenough et al. 2005) of mafic and felsic rocks from (a), island arc tholeiites (IAT) compared to (b) average ocean-island basalts (OIB) and mid-ocean ridge basalts (MORB). Note the different vertical scales in the two diagrams. The shaded areas are typical of the slopes and ranges of REE abundances in a given arc suite; they are not intended to represent fields of arc compositions. Island arc tholeiites have flat REE profiles and minor light REE depletion. Arc rocks typically show moderate light REE enrichment, but much less pronounced than OIB. Note the Eu anomaly in felsic rocks that is attributed to plagioclase fractionation. These gently sloping profiles are consistent with generation of magma in the shallow (spinel lherzolite) mantle (< 50 km depth) rather than a deep (garnet lherzolite) mantle.

REE is divided by the concentration of that element in chondrite, which is thought to reflect the composition of the early Earth. This results in smooth patterns that facilitate comparisons among samples and between two suites. The resultant chondrite-normalized rare-earth-element plot (note that the y axis is dimensionless) allows an analysis of the enrichment (or depletion) in each lanthanide element relative to the same standard reference, in this case, that of the early Earth (Fig. 7). Analysis of these plots focuses on two different aspects. First, as REE elements are equally incompatible during fractionation of the early crystallizing phases, the slope on the REE diagram (as represented by normalized La/Lu) is virtually unaffected by fractionation and so represents their relative abundances in the source rock. An overall envelope around the REE data from a given suite may therefore yield valuable information of the chemistry of that source. Second, total REE (ZREE) should increase until the latest stages of fractionation (Fig. 7a), and suites, derived from the same source and related by fractionation, should yield parallel profiles. For crystal fractionation to be a viable model, samples that have higher ZREE should have higher abundances of incompatible elements and so the REE profiles are generally checked against abundances of elements such as Zr and Nb.

Island arc tholeiites exhibit relatively flat REE profiles, with minor depletion in light rare-earth-elements LREE). These profiles are broadly similar to MORB (although MORB has more pronounced LREE depletion) suggesting derivation from a similar source, i.e. the depleted mantle. In contrast, calc-alkalic basalts show moderate degrees of light rare-earth enrichment, although they are not as enriched as alkalic or plume-related basalts, suggesting derivation from a mantle source enriched in these elements relative to the source for MORB or IAT.

Tholeiitic and calc-alkalic lavas are both characterized by flat heavy REE (HREE) profiles. These profiles imply a source in the shallow (spinel lherzolite) mantle (i.e. < 50 km depth) rather than a deeper (garnet lherzolite) mantle. Garnet preferentially incorporates HREE over LREE, so that a steepened REE slope (i.e. higher La/Lu) will result if either fractional crystallization of garnet occurs during cooling, or if garnet remains in the residuum during partial melting (Fig. 7b). The effect of garnet on REE profiles contrasts with other silicates, the fractionation of which increases ZREE but does not change the slope of REE profiles. In addition, the flat HREE patterns are also a strong argument that the magmas are not directly

derived from melting of the subducted slab, because oceanic lithosphere subducted to 110 km depth would be metamorphosed to eclogite (a garnet-omphacite bearing metamorphic rock).

Plagioclase incorporates more Eu than the other REE because, unlike other lanthanides, which are predominantly trivalent, Eu is predominantly divalent (Eu^{2+}/Eu^{3+} depends on fO_2) and so can be incorporated into the Ca^{2+} site in the plagioclase structure. If fractionation of plagioclase occurs during cooling, the increase in Eu concentration lags behind the increases in other REE, resulting in a negative "kink" in chondrite-normalized REE patterns (Fig. 7b), known as a "negative europium anomaly". The extent of the anomaly increases with fractionation, and so is very pronounced in felsic rocks as can be seen by comparing normalized Eu abundance with a hypothetical Eu value obtained by extrapolating a hypothetical line from neighbouring elements (dashed line, Fig. 7b). The presence of a negative Eu anomaly in many tholeiitic and calc-alkalic volcanic arc suites is consistent with plagioclase fractionation, which is typical of processes in crustal magma chambers and matches field and petrographic evidence of the abundance of plagioclase phenocrysts.

When trace elements and REE elements are considered together, it is evident that arc systems are complex and magma compositions represent interplay of a large number of factors, including magma mixing, crustal contamination, crustal assimilation, and fluid transport. These complexities are revealed if ratios between incompatible trace elements in basaltic rocks are studied. If arc liquids evolve by simple fractionation, ratios such as La/Nb and Zr/Nb remain constant because La, Zr and Nb are (approximately) equally incompatible elements. Geochemical studies from most arc magmas show that this is rarely the case, and while they do not negate the possibility that fractional crystallization played an important role, they also indicate that other processes are responsible for these variations, such as source heterogeneities, magma mixing or crustal assimilation.

Arc Magmas on Discrimination Diagrams

Since the early 1970s, a plethora of geochemical discrimination diagrams have been published utilizing the varying behaviours of compatible and incompatible trace elements to distinguish magmas by type (alkalic, tholeiitic, calc-alkalic) and by tectonic setting (arc, within plate, etc), and also to constrain the chemistry of the magma source. In this approach, incompatible elements are subdivided on the basis of their ionic potential (charge/ionic radius) into *high-field-strength* elements and *large ion lithophile* (LIL) elements. High-field-strength elements are relatively small incompatible elements that have a high charge density (e.g. Ti^{4+}, Zr^{5+}) and high ionic potential; other HFS elements include Th, U, Hf, Nb, Y, Ta and REE. They are typically insoluble in H_2O-rich solutions. Large ion lithophile elements, however, have low charge and low ionic potential and are soluble in water-rich solutions (e.g. K, Rb, Cs, Ba, Sr). As H_2O plays a key role in the genesis of arc magmas, the contrasting behaviour of LIL and HFS is crucial to understanding their petrogenesis and many arc magmas have high LIL/HFS elemental ratios (Pearce 1996).

Although the foundation for many discrimination diagrams (e.g. Figs 8-10) is basically empirical (they are based on data from volcanic rocks in known tectonic settings), and the reasons for these variations are not fully understood, they do provide some general constraints for the origin of arc basalts.

High-Field-Strength Elements

The first type of discrimination diagram relies on HFS elements. For example, on the Zr/Ti vs Nb/Y plot (Fig. 8a; Winchester and Floyd 1977; modified by Pearce 1996), fractionation of early crystallizing phases such as olivine, augite and plagioclase does not significantly affect either the Zr/Ti or Nb/Y ratio because all four elements are incompatible in these phases. However, fractionation of amphibole or magnetite will drive liquids toward intermediate and felsic compositions. As noted by Pearce (1996), this diagram is a proxy for the total alkalies vs silica classification diagram, where Nb/Y measures the degree of alkalinity and Zr/Ti is an index of fractionation. However, the HFS trace-element diagram has the considerable advantage in that the elements selected are relatively immobile during secondary processes (e.g. weathering, low-grade metamorphism), in contrast to the alkalies and silica.

The high Nb/Y of alkalic suites can be attributed to the presence of residual garnet which retains Y in the source rock. Thus, the relatively low Nb/Y in calc-alkalic and tholeiitic arc basalts is consistent with REE evidence suggesting derivation from a shallower (spinel lherzolite) mantle than alkalic basalts. Similar principles can be seen in other discrimination plots (Figs. 8b, c) which emphasize the low Ti, Zr and Zr/Y in arc magmas compared to within-plate magmas, as is apparent on the TiO_2 vs Zr and the Zr/Y vs Zr diagrams (Pearce and Norry 1979; Pearce et al. 1981).

As HFS elemental ratios (e.g. Zr/Y, Fig. 8c), Ti/Y and Nb/Y (Fig. 8d) are insensitive to fractionation in the shallow mantle, variations in these ratios may reflect heterogeneities in the mantle source. The behaviour of Y and Yb, however, changes depending on depth in the mantle. The elements are incompatible in the shallow (spinel lherzolite) mantle, but are compatible in the deep (garnet lherzolite) mantle, where they are retained in garnet during partial melting. Therefore, the lower Ti/Y for arc basalts compared to within-plate basalts (WPB) suggests an

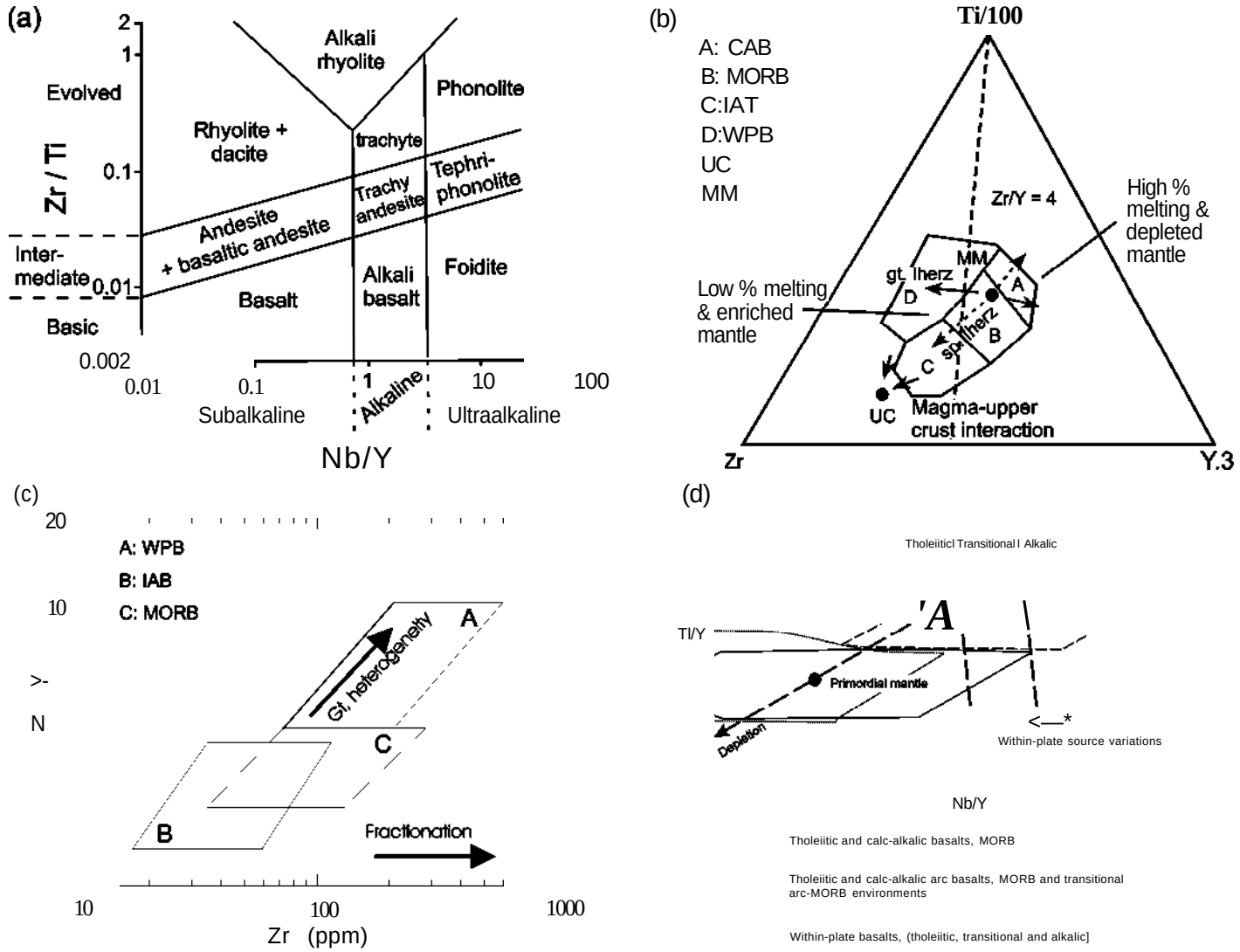

Figure 8. Various Ti-Y-Zr-Nb discrimination diagrams as follow: (a) bivariate Zr/Ti vs Nb/Y diagram (after Winchester and Floyd 1977; Pearce 1996); (b) triangular Ti/100-Y*3-Zr diagram (after Pearce 1982). CAB = calc-alkali basalt; MORB = mid-ocean ridge basalt; IAT = island arc tholeiite; WPB = within plate basalt.; UC = average upper crust; MM = average N-MORB mantle; (c) log-log plot of Zr/Y vs Zr (after Pearce and Cann 1973); (d) log-log plot of Ti/Y vs Nb/Y (after Pearce 1982).

origin in the shallow spinel lherzolite mantle.

Fractionation and Partial Melting

A second type of discrimination diagram focuses on elements that have contrasting behaviours during igneous processes. The Cr-Y discrimination diagram (Pearce 1982; Fig. 9) is an example of a compatible element (Cr) plotted against an incompatible HFS element (Y) and can monitor the extent of fractionation and partial melting. According to Wood (1979), Cr and Y exhibit limited variability in the mantle, so that variations in basalts can be attributed to differences in degrees of partial melting and fractional crystallization. Because Cr is a highly compatible element but Y is incompatible, the fractionation trend on this graph is nearly parallel to the Cr axis. The diagram successfully discriminates between tholeiites formed in arc environments (IAT) and MORB. Island arc tholeiites have lower Y than MORB for a given Cr concentration. Petrogenetic modelling using these elements shows that variations in IAT can be explained by between 15-40% partial melting followed by fractionation of mafic phases. Clearly MORB rocks are, on average, less fractionated than IAT.

Mantle Heterogeneity and Source

A third type of discrimination diagram is based on the geochemical differences between LIL and HFS incompatible elements and the high LIL/HFS ratio of arc magmas. The concentrations of HFS elements are not appreciably affected by processes that cause mantle heterogeneity. The LIL incompatible elements (e.g. Th and LREE) are soluble in fluids derived from the subduction zone; therefore, they are enriched in the mantle wedge and the melts derived from this mantle inherit

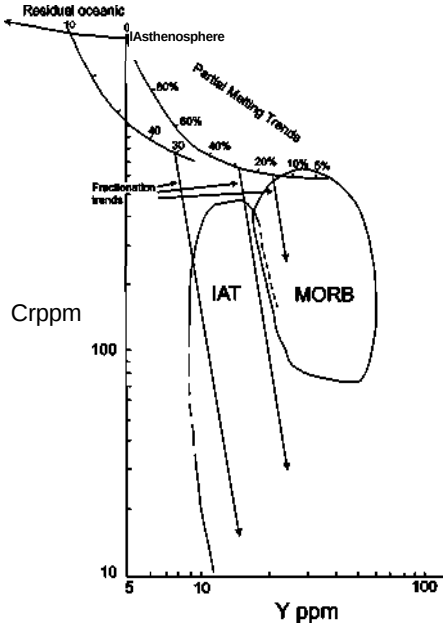

Figure 9. Log-log plot of Cr vs Y (after Pearce 1982). IAT: Island arc tholeiites; MORB: Mid-Ocean Ridge Basalts.

that enrichment. Although there is a consensus that arc magmas are LIL-enriched, there is some debate as to the extent of depletion in HFS elements. At one extreme, McCullough and Gamble (1991) and McCullough (1993) argue that HFS element concentrations of the arc magmas are similar to MORB and so are not significantly depleted. In contrast, others (e.g. Saunders and Tarney 1984; Saunders et al. 1991) point out that the oxidizing environment (caused by the addition of water to the mantle wedge) stabilizes minerals such as titanite, rutile, ilmenite and hornblende, which contain high abundances of HFS elements (Zr, Ti, Nb, Hf, Ta). These minerals remain in the residue during partial melting, so the HFS elements are depleted in arc magmas. Another possibility is that low HFS elemental abundances reflect contamination with continental crust that was previously depleted in HFS elements, and so magmas contaminated by it would inherit this depletion. Although such contamination has been documented in several localities, this model does not address how the crust originally became depleted in HFS elements.

On elemental ratio plots such as Th/Yb or Ce/Yb vs Ta/Yb (Figs. 10 a, b; Pearce 1982), the vertical axis detects subduction components so that arc-related rocks plot above the typical mantle values. Calc-alkalic basalts (CAB) have higher Ce/Yb and Th/Yb than arc tholeiitic basalts. These traits are further evidence of the chemical effects of fluids derived from the subduction zone carrying Ce and Th to the mantle wedge source region of arc basalts (Pearce 1996). Whereas MORB and WPB plot near the mantle array, arc basalts (both CAB and IAT) have lower Ti/Y and Ta/Yb than rift-related basalts and typically plot above the mantle array.

The Hf-Th-Ta diagram (Fig. 10c; Wood et al. 1979) also identifies the influence of subduction components in the trace-element chemistry. As arc magmas are enriched in Th, and are especially depleted in Ta (Pearce 1996), they plot nearer the Hf-Th join than MORB or within-plate basalts. Calc-alkalic basalts have higher Th than IATs and so plot closer to the Th apex of the discrimination diagram (compare D1 and D2). As arc systems mature, they also become more enriched in LREE relative to HREE. This tendency is identified on the La/Yb vs Th/Yb diagram (Fig. 10d, after Condie 1989) where primitive island arcs have lower ratios than continental (Andean) arcs.

Tectonic Setting

Other discrimination diagrams are used to elucidate the tectonic setting. The Ti-Zr plot (Fig. 11) is sensitive to crystal fractionation in arc and within-plate suites (Pearce and Norry 1979). Fractionation of most early-crystallizing phases (such as olivine, cpx, opx, plag) results in an increase in these two elements. However, fractionation of magnetite causes depletion in Ti, and fractionation of amphibole or biotite may cause depletion in Ti and Zr (see partition coefficients in Table 2). Fractionation vectors (Fig. 11) show that differentiated arc lavas (both tholeiitic and calc-alkalic) have lower Ti and Zr than differentiated within-plate lavas.

Pearce et al. (1984) showed that arc-related felsic magmas have lower Rb, Y, Nb, Ta and Y than within-plate or ocean-ridge granites (Figs. 12 a, b). Petrogenetic models of compositional trends of arc granites on the Rb-(Y+Nb) plot indicate that source rocks are enriched in Rb (presumably from fluids derived from the subduction zone). The authors note that fractionation vectors for amphibole in intermediate and felsic rocks enhance the vertical trend, facilitating distinction between arc and within-plate granites.

Some Limitations to the use of Discrimination Diagrams

While these diagrams have been a valuable tool in fingerprinting magma type and tectonic settings, there are some limitations and inconsistencies in their application. First, these diagrams assume that the abundances of these elements in a given rock sample are essentially unchanged since the time of crystallization. This assumption generally holds because HFS elements are typically insoluble in water-rich solutions and are most concentrated in stable accessory phases such as zircon, ilmenite and titanite. However, dissolution of these phases can occur under certain conditions (e.g. rocks subjected to hydrothermal alteration or carbonatization (Hynes 1980)) and samples from rocks so affected yield spurious results.

Second, there are some inconsistencies among the diagrams themselves. For example, on the Zr/Y vs Zr plot, within plate basalts (e.g. continental rift-related basalts) are classified by $Zr/Y > 4$. If one plots this line on the Zr-Ti-Y discrimination diagram, it is evident that some rocks with $Zr/Y > 4$ plot in the IAT, CAB or MORB fields (Fig. 8b, c). It is important to remember that these diagrams are pro-

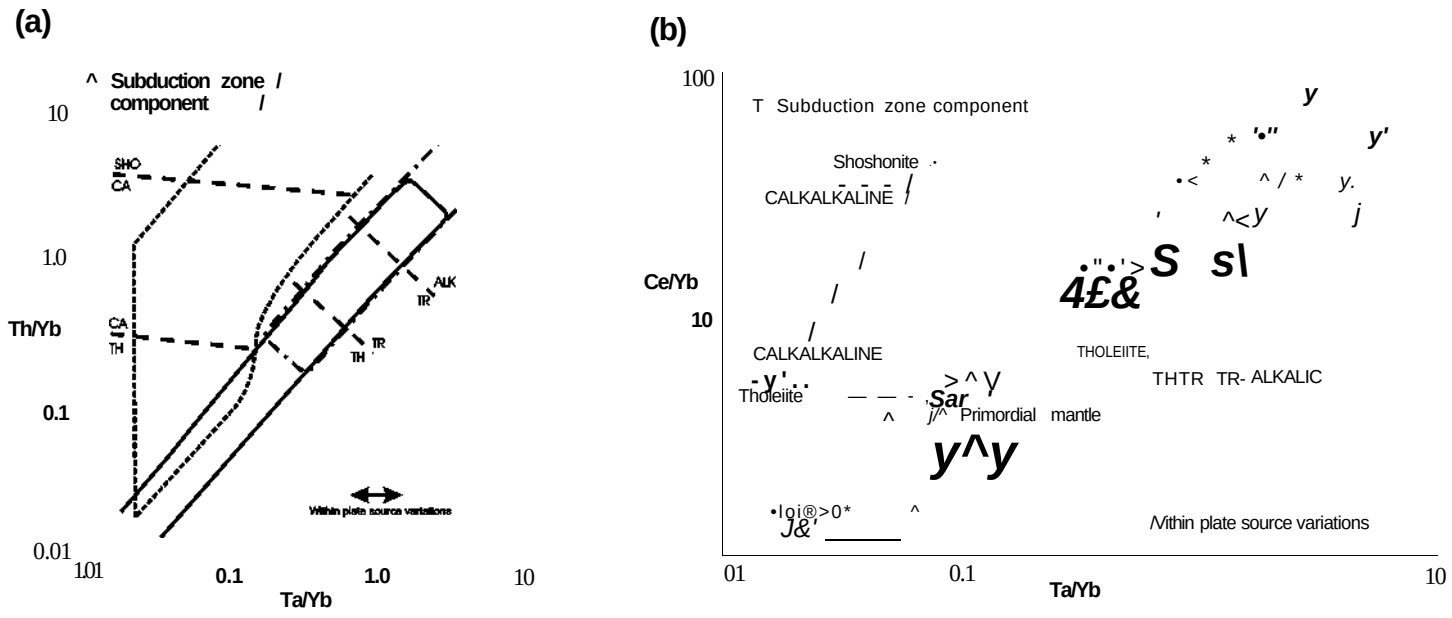

Transitional volcanic arc basalts, (alkalic arc basalts, tholeiitic arc basalts, tholeiitic MORB)

Tholeiitic MORB, transitional MORB, tholeiitic arc basalts, within-plate basalts (alkalic, tholeiitic, transitional)

Transitional MORB, alkalic arc, within-plate (alkalic, tholeiitic, transitional)

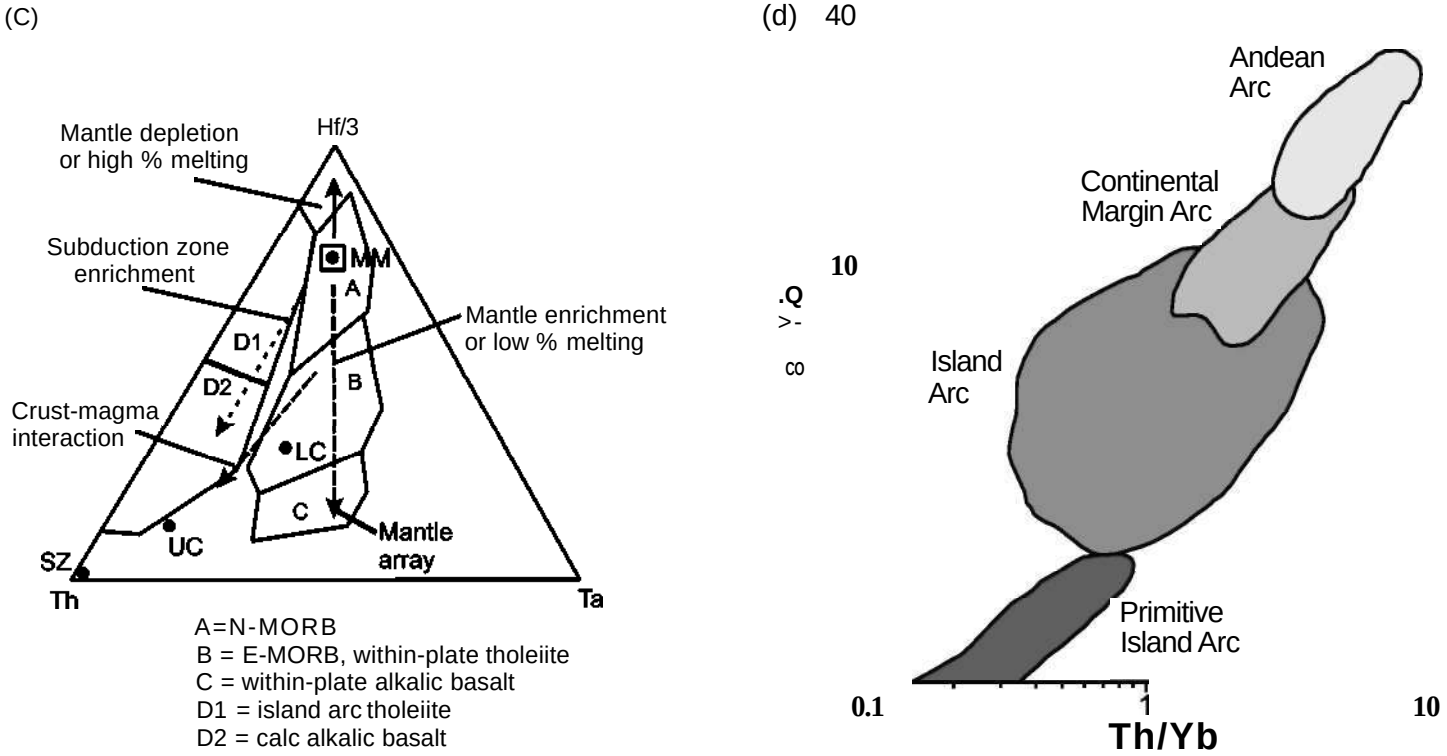

Figure 10. Diagrams illustrating the use of trace elements to identify subduction components: (a) log-log plot of Th/Yb vs Ta/Yb (after Pearce 1982); (b) log-log plot of Ce/Yb vs Ta/Yb (after Pearce 1982); (c) triangular Hf/3-Ta-Th diagram (after Wood et al. 1979), MM = NMORB mantle source; UC = upper crust; LC = lower crust; SZ = subduction component; (d) log-log plot of La/Yb vs Th/Yb (after Condie 1989).

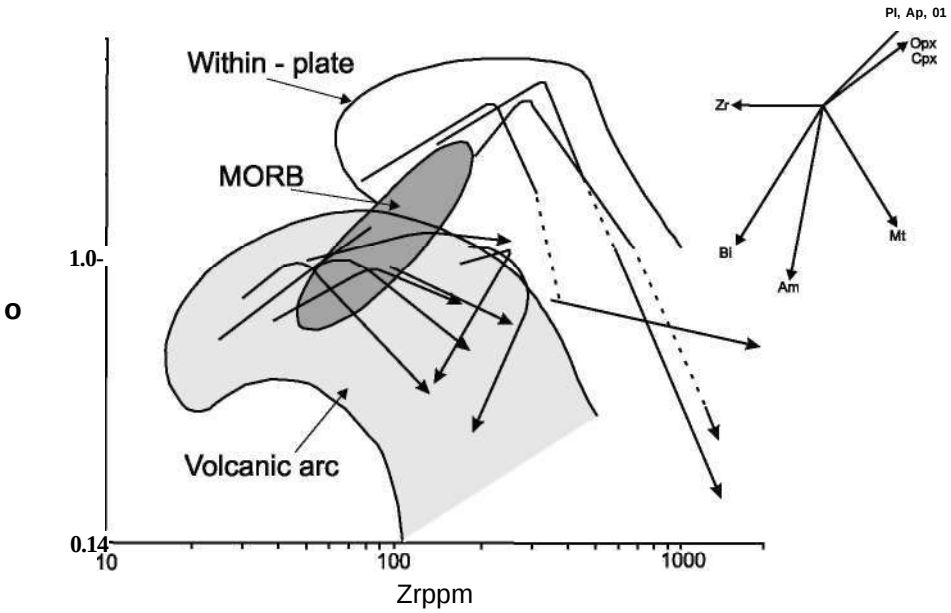

Figure 11. Log-log plot of TiO2-Zr (after Pearce and Norry 1979; Pearce 1982) showing fractionation trends of various arc and within-plate suites. Vectors associated with fractionation of olivine (Ol), orthopyroxene (Opx), clinopyroxene (Cpx), plagioclase (Pl) apatite (Ap), magnetite (Mt), amphibole (Am), zircon (Zr), and biotite (Bi) for F = 0.5 are from Pearce (1982).

jections that look at a very restricted compositional plane and so a variety of diagrams must be employed to be sure of consistency in interpretation.

Major-Trace-Element Decoupling

Perhaps the most important, but under-appreciated, limitation to the use of discrimination diagrams is that trace elements are highly sensitive to a variety of petrological processes, whereas major element variations are primarily controlled by phase equilibria. The net result is that major and trace elemental behaviour may "decouple", leading to conflicting results for tectonic settings for volcanic rocks (see Spandler et al. 2003; Leibscher 2004).

Consider, for example, a typical arc plumbing system that has magma chambers of the same starting composition, but of varying size connected by a set of conduits (Fig. 13). There is abundant field and petrological evidence to show that magma chambers are open, rather than closed systems and that magma is pumped along conduits between magma chambers in response to pressure variations in the system, much as water is pumped through a municipal water system. If relatively small increments of magma from a large, more mafic chamber (Y) are repeatedly pumped into a smaller, more silicic chamber (M), then major and trace elements will behave differently. A standard phase diagram of a basaltic magma (X) undergoing olivine-enstatite fractionation shows that the magma composition in each chamber will be driven down the olivine-enstatite reaction curve (Fig. 13), where olivine reacts with the liquid, as enstatite precipitates. Although there is a tendency for the bulk composition of magma chamber M to migrate incrementally toward the composition of invading magma Y, this is immediately counterbalanced as magma M enters the pyroxene stability field, thereby resulting in rapid crystallization of pyroxene that drives the liquid away from the enstatite composition back toward the pyroxene-plagioclase cotectic (Boudreau and McBirney 1997). Major element chemistry, therefore, is only moderately affected by the invading magma. Trace elements, on

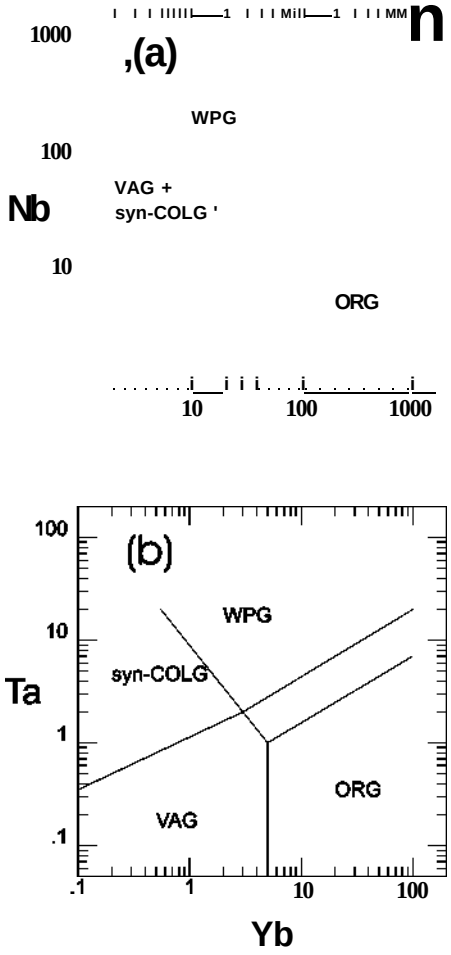

Figure 12. Discrimination diagrams for felsic rocks: (a) log-log plot of Nb vs Y; (b) log-log plot of Ta vs Yb (after Pearce et al. 1984). Abbreviations are: syn-COLG - syn-collision granite, ORG - orogenic granite, VAG - volcanic arc granite, and WPG - within plate granite.

the other hand, are not controlled by this process, and so would plot on mixing curves between the two end member compositions Y and M.

Spider Diagrams

Geochemical data are also presented on normalized multi-element diagrams, in which the abundances of a range of elements are compared with a reference source, known as *spider diagrams* (Figs. 14 a, b). Many spidergrams compare the trace element content of samples with those of a number of diverse reservoirs that could represent potential sources, such as MORB, depleted

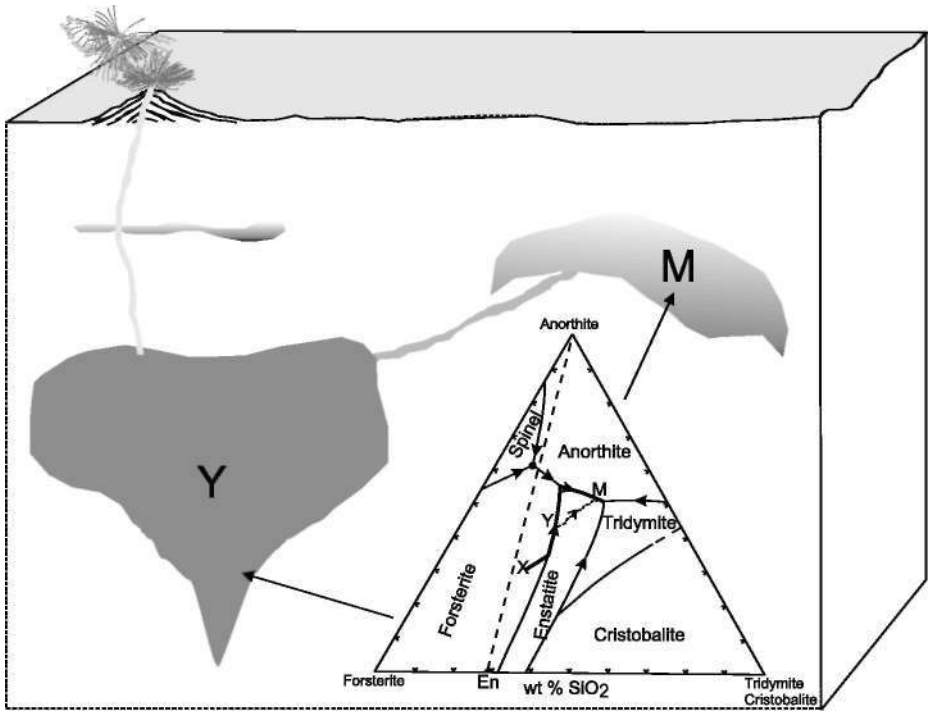

Figure 13. Hypothetical arc plumbing system with chambers of the same starting composition but of different sizes. See text for details. If an increment of magma of composition Y is introduced into a chamber, the resident magma moves into the stability field of enstatite, which then precipitates, driving the liquid composition away from enstatite. Repeated injections into the chamber of magma of composition Y will cause the magma to follow a jagged path (dotted line) in the direction of the arrow (Y to M). However, X-Y, and X/Y vs Z/Y trace element diagrams would plot on linear mixing lines, and X/Y vs W/Z diagrams would plot on hyperbolic mixing curves (see Appendix 1, Figs. A1b to e).

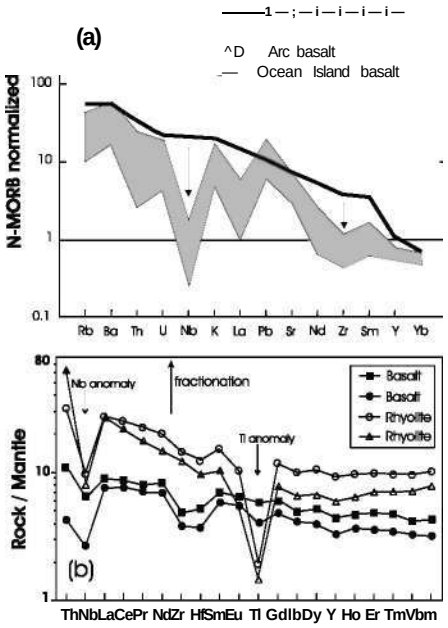

Figure 14. Spider-diagrams: (a) Typical MORB-normalized patterns for arc basalts compared with ocean-island basalts (modified from Tatsumi 2005). (b) Typical mantle-normalized patterns for arc mafic and felsic rocks. Normalizing values after Sun and McDonough (1989). The arrows identify elements such as Zr, Nb and Ti, which have anomalously low values typical of arc magmas.

mantle (DM, the mantle from which basalt has been extracted), and enriched mantle (EM, mantle that has been extensively metasomatized). The elements are ordered with increasing compatibility from left to right. Spider diagrams are analyzed in a similar fashion to chondrite-normalized diagrams. The data are normalized relative to a candidate reservoir. If basaltic suites are being studied, typically they are either compared with MORB or with a mantle reservoir (e.g. DM or EM). An envelope around the data is compared with that of the candidate mantle reservoir and yields valuable evidence about the source of the magma. Variations within the data set provide information about the extent of fractionation. Fractionated magmas derived from the mantle reservoir, for example, ideally should yield a set of parallel profiles within the envelope.

Mafic to intermediate arc rocks typically exhibit jagged MORB-normalized patterns, and most notably, a negative Nb anomaly relative to Th or La (Fig. 14a, e.g. see Sun and McDonough 1989). In contrast, mafic rocks from non-arc settings are characterized by relatively smooth MORB-normalized patterns (especially ocean-island basalts) and some have positive Nb anomalies. Jagged patterns are also evident in mantle normalized plots for mafic and felsic rocks generated in arc environments (Fig. 14b). In essence, the jagged patterns show the same LIL element enrichment relative to HFS elements (see Nb, Ti, Zr, and Ta), which is evident in several discrimination diagrams. Although these same traits can be recognized on standard discrimination diagrams, the advantage of these plots is that trends can be shown and compared for many elements on the same diagram. Although mafic magmas in both arc and non-arc settings are derived from the mantle, these diagrams also identify the distinctive high LIL/HFS ratio of arc magmas. When the metasomatized mantle wedge melts, LIL elements strongly partition into the melt, whereas HFS elements preferentially remain in stable accessory minerals. Melts derived from this metasomatized mantle wedge are therefore enriched in LIL relative to HFS elements (e.g. Miškovic and Francis 2006). Tatsumi and Kogiso (2003) have used this approach to propose that the dehydration of subducted sediments and oceanic crust released water and LIL elements into the mantle wedge. This hypothesis is supported by boron and beryllium studies. Boron

and ^{10}Be are enriched in sediments, but escape very easily upon entering the subduction zone. Many modern arc volcanic rocks have elevated concentrations in these elements, which can only be derived from subduction of recent sediments (e.g. Morris et al. 1990; Morris and Ryan 2004).

The origin of the jagged mantle-normalized patterns in felsic magmas could arise in several ways. As fractionation generates a series of parallel trends, these patterns could be derived from fractionation of a more mafic parent. Alternatively, these features can be inherited from mafic magma derived from metasomatized mantle, and the differentiated products from such magma reproduce the jagged pattern. Supporting evidence for this hypothesis is gained from the analyses of xenoliths (retrieved from kimberlite bodies) that are derived from the mantle beneath some continental arcs. These data indicate that the mantle source may have suffered extensive and long-term metasomatism. Alternatively, as continental crust is primarily formed by earlier arc magmatism, they may reflect partial melting of continental crust that was mostly generated by earlier arc activity. In this case, the jagged pattern is inherited from the crustal source, rather than a reflection of coeval subduction.

Intermediate to felsic magmas in arc settings are also depleted in HFS elements relative to felsic magmas from within-plate settings. However, there is considerable debate about the origin of intermediate to felsic magmas in arc settings, and their origin may vary from one arc to another (Gill 1981; Carmichael 2002). As these magmas tend to be most dominant in mature arcs with thick continental crust, such as the Andes, much discussion focuses on whether the thickened crust allows more scope for fractionation, or whether the crust supplies a direct chemical contribution (see Carmichael 2002, and references therein). In some instances it is argued that this signature is inherited from basalts by fractional crystallization. In others, the felsic composition is attributed to partial melting of the crust or contamination of mafic to intermediate lavas by the crust. Since this crust is depleted in HFS elements, it is difficult to distinguish between these hypotheses using trace-element geochemistry alone. Given that the average continental crust is very similar in composition to calc-alkaline andesites (e.g. Taylor 1995), resolution of the problem has fundamental implications for understanding the evolution of the crust. The following section discusses how radiogenic isotopes, particularly Sm-Nd isotopic studies, can help distinguish among these various possibilities.

ISOTOPIC CHARACTERISTICS

In addition to their use in dating rocks and minerals, certain types of isotopes can be used as tracers to yield information about the original source material from which a volcanic rock was derived. Several isotopic methods are used, including Rb-Sr, and Sm-Nd and U-Pb. Rubidium-Sr and Sm-Nd are commonly considered together.

Rb-Sr and Sm-Nd Isotopes

Rubidium has an ionic radius of 1.48C, which is similar to K (1.33C). As a result, Rb is common in K-bearing minerals, including micas and K-feldspars. As an alkali element, Rb strongly partitions into crustal rocks, so that Rb/Sr is *higher* in crustal rocks than in the bulk Earth and *higher* in the bulk Earth than in the depleted mantle source. Therefore, $^{87}Sr/^{86}Sr$ increases more rapidly in the crust than it does in the bulk Earth, and more rapidly in the bulk Earth than it does in the depleted mantle.

Variations in Sm/Nd ratios in crustal rocks are mostly inherited from their mantle sources (see DePaolo 1988). When the mantle melts, all LREEs tend to concentrate in the magma rather than in the remaining, now *depleted mantle*. Although Sm and Nd are both lanthanides and have the same valency (+3), Nd has a lower atomic number (60), and is slightly larger than Sm. Thus, it is slightly more concentrated than Sm in magmas leaving the depleted mantle (in accordance with Goldschmidt's rules). The larger Sm ions are slightly more concentrated than Nd in mantle minerals. Thus, the average Sm/Nd is *lower* in the crust than it is in the depleted mantle (0.2 and 0.5 respectively, Fig. 15a). Therefore, the decay of ^{147}Sm to ^{143}Nd results in a more rapid increase in $^{143}Nd/^{144}Nd$ in the depleted mantle than in the bulk Earth, and a more rapid increase in the bulk Earth (average Sm/Nd = 0.32) than in the crust (Fig. 15a). Consequently, the Sm-Nd isotopic characteristics of magmas generated in the crust and the depleted mantle are very different. However, in the case of the Rb-Sr system, the crust is *enriched* in the radioactive component, whereas in the case of the Sm-Nd system, the crust is *depleted* in the radioactive component. Upon melting, magmas acquire the $^{87}Sr/^{86}Sr$ and $^{143}Nd/^{144}Nd$ ratio of their source, and so this negative relationship also exists in magmas. Magmas formed by melting the depleted mantle will have *lower* initial $^{87}Sr/^{86}Sr$ and *higher* initial $^{143}Nd/^{144}Nd$ ratios than those produced by melting the crust.

On a plot showing typical Nd-Sr isotopic variations in modern arc volcanics the negative relationship between $^{87}Sr/^{86}Sr$ and $^{143}Nd/^{144}Nd$ initial ratios is apparent (Fig. 16). Some arc suites, such as the Aleutians, New Britain, South Sandwich and the Marianas have values that are more depleted than the bulk earth (i.e. higher initial $^{143}Nd/^{144}Nd$ and lower initial $^{87}Sr/^{86}Sr$) and are almost as depleted as MORB. Other arcs, however, are enriched in these isotopes (i.e. lower initial $^{143}Nd/^{144}Nd$ and higher initial $^{87}Sr/^{86}Sr$ than the bulk earth), suggesting that subducted oceanic sediments may have influenced the composition of the magma. As the data lie close to a mixing line between depleted mantle and

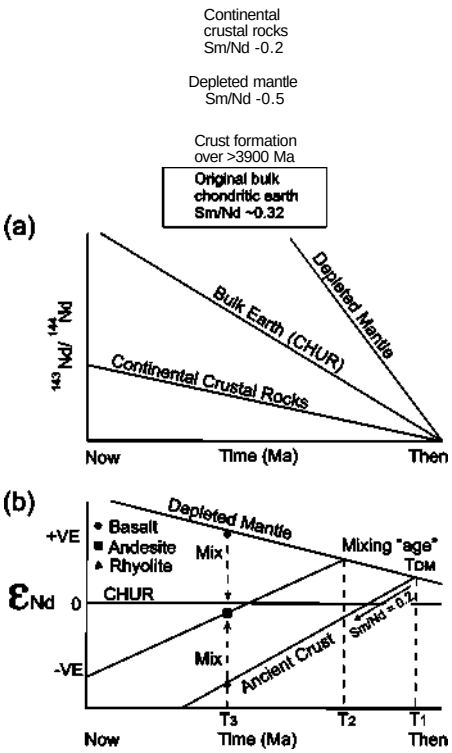

Figure 15. (a) Diagram showing how the $^{143}Nd/^{144}Ndi$ initial ratio changes with time. The depleted mantle preferentially retains Sm over Nd so that its Sm/Nd ratio (~0.5) is greater than that of bulk Earth (CHUR) (~0.32) and the continental crust (~0.2). Therefore, $^{143}Nd/^{144}Nd$ (represented by E_{Nd}) increases more rapidly in the depleted mantle than in either the crust or the bulk Earth, and so evolves toward positive values, whereas the crust evolves toward negative E_{Nd} values, measured relative to bulk Earth or CHUR. (b) The change in the E_{Nd} value of a sample with time depends on its Sm/Nd ratio. This ratio can be measured accurately, so that the evolution of E_{Nd} with time can be determined, and is shown as a growth line. The interception of this growth line with the depleted mantle curve represents the age when the sample was in isotopic equilibrium with the depleted mantle (DM), and is known as the depleted mantle model age, or T_{DM} (DePaolo 1981a, b; 1988). See text for details.

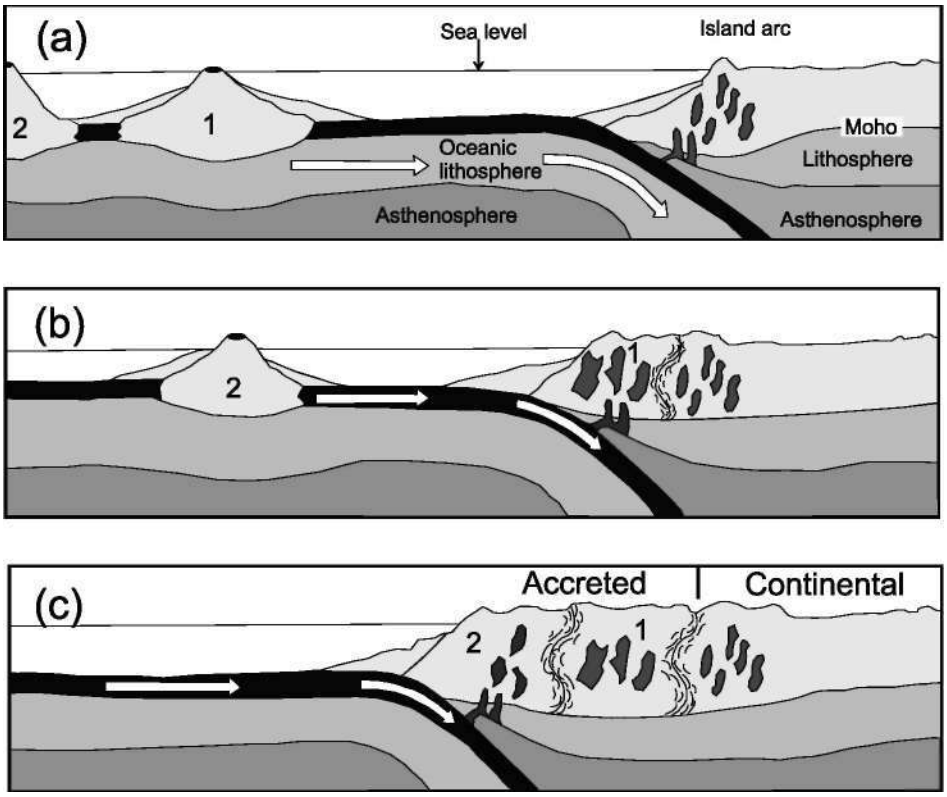

Figure 16. Schematic diagrams illustrating terrane accretion at a convergent continental margin: (a) Subduction under the continental margin results in the development of a continental (Andean-style) arc; (b and c) Outboard oceanic terranes are swept into the subduction zone and accreted to the continental margin. After each collision, a new subduction zone forms outboard from the collision zone. The basement and mantle lithospheres become recycled, and are isotopically distinct from the continental arc crust. The line in (c) shows the boundary between magmatism sourced from recycled ancient continental lithosphere (right) and magmatism sourced from recycled juvenile accreted lithosphere.

sediments, a permissible interpretation is that arc magmas are sourced in a depleted mantle (similar to MORB) that has been variably influenced by fluids derived from subducted sediments or crust (about 5% contamination, Fig. 16).

These isotopic data can also be used to determine if the magmas were recently derived from the mantle or from recycling of ancient crust. Changes in the isotopic signature of the depleted mantle and the average or "bulk Earth" with time are well constrained (Fig. 15). The isotopic signature of the crust, however, depends on how long ago it separated from the mantle, i.e. the greater the time interval, the bigger the differences in Rb/Sr and Sm/Nd ratios. Compared to newly formed crust, older crust has a much greater difference between its isotopic signature and that of the depleted mantle from which it originated.

One of the most challenging tasks of arc magmatism is to evaluate how intermediate to felsic magmas are derived, i.e. by fractionation of a more mafic parent, by crustal melting or by some combination of these two processes. Samarium-Nd isotopic studies can help reveal the relationship between coeval basalts and rhyolites in arc magmas. Fractionation of the basaltic magma does not change its isotopic characteristics, and rhyolite derived from it inherits these same characteristics. In contrast, intermediate to felsic magmas derived by melting old crust will have Sm and Nd isotopic

characteristics of the crust and will be very different from coeval, mantle-derived basaltic magma and its differentiates. In northeastern Japan, the basaltic and rhyolitic rocks generally have different Sm-Nd isotopic compositions, suggesting they are not co-magmatic, and the rhyolites reflect partial melting of the crust (e.g. Tatsumi 2005).

These isotopic methods for deducing the nature of the source rock assume that: 1) the isotopic evolution of the depleted mantle is known, 2) the samples' Rb/Sr or Sm/Nd ratios have not been modified by coeval or subsequent intra-crustal processes (e.g. assimilation of host rock, fractionation of REE-bearing phases, hydrothermal activity), 3) a crustal Rb/Sr or Sm/Nd ratio was acquired during, or very soon after, the sample was emplaced in the crust, and 4) all the material in the sample was derived from a single event in the mantle (e.g. Arndt and Goldstein 1987)

In many cases, these assumptions break down in the Rb-Sr system. Because Rb is an alkali metal, and Sr an alkali earth metal, they behave very differently in the crust, and the Rb/Sr can be affected by a wide variety of crustal processes including weathering, diagenesis and metamorphism. In contrast, the decay of samarium (Sm), to neodymium (Nd), provides one of the best tracers for tectonic processes (e.g. DePaolo 1981a, b; 1988). Samarium and neodymium are both light "rare earth" elements with similar ionic radii and valencies (+3), so they have similar chemical properties and thus Sm/Nd is rarely affected by crustal processes.

The differences in the $^{143}Nd/^{144}Nd$ ratios of crustal and mantle rocks are relatively small. For convenience, a parameter, e_{Nd}, is defined which reflects the *difference* between the $(^{143}Nd/^{144}Nd)_o$ in the sample and that of "bulk Earth" at the time the rock crystallized (DePaolo 1988). In this scheme, £$_{Nd}$ for the bulk Earth at any time is set at zero. As $^{143}Nd/^{144}Nd$ increases more rapidly in the depleted mantle and less rapidly in the crust compared to the bulk Earth, over time the depleted mantle has evolved toward more positive E_{Nd} values, while the crust has evolved toward more negative values. The evolution of the crust produces a growth line with a predictable slope because the Sm/Nd ratio of crustal rocks is typically about 0.2 (Fig. 15b).

Because of their contrasting growth lines, E_{Nd} values can be used to distinguish between magmas derived from a depleted mantle source and those derived from the melting of an ancient crustal one (Fig. 15b). This is particularly important in the understanding of the genesis of intermediate and felsic rocks in arc systems. In contrast to magmas formed by partial melting of the crust, andesites and rhyolites derived from fractional crystallization of a basaltic magma will each have the same E_{Nd} value as the coeval basalt because these isotopic ratios are not affected by fractional crystallization. Samarium-Nd isotopic studies can also identify intermediate magmas formed by mixing of mafic and felsic "end-members", which should have E_{Nd} values that lie between those of the mafic and felsic parents. The degree of crustal inheritance in the genesis of magma can also be assessed because most crustal processes do not change the Sm/Nd ratio (e.g. Murphy et al. 1996).

In practical terms, these principles are used in reverse. The isotopic analysis of a rock sample reveals the present-day value of E_{Nd} The growth line, representing the rate of change in this value with time, can be determined, so that the time when E_{Nd} would have had the same value as that of the depleted mantle can be deduced from the intersection of the growth line with the depleted mantle curve. This date is referred to as the depleted-mantle model age (or T_{DM}). If the four assumptions listed by Arndt and Goldstein (1987) are satisfied, this is the time when the sample had the same isotopic signature as its depleted mantle source. For arc magmas, the T_{DM} age represents the time when the source rock for the magmas was itself extracted from the mantle (Fig. 15).

Most crust is derived, either directly or indirectly, from the depleted mantle reservoir. As a result, the value of E_{Nd} for a sample compared to that of the depleted mantle at the time of the rock's crystallization, i.e. its *initial* E_{Nd} value, is crucial to tectonic interpretations. Volcanic rocks with initial E_{Nd} values similar to those of the depleted mantle must have been derived from the depleted mantle reservoir at, or about, the time of their formation, and are therefore considered "juvenile". For a juvenile rock, its T_{DM} age will be similar to its crystallization age. Conversely, volcanic rocks with E_{Nd} values well below those of the depleted mantle at the time of their crystallization are generally interpreted to have been derived from the melting of ancient crust. The time at which this ancient crust was itself separated from the mantle can be determined from the intersection of its growth line with that of the depleted mantle (Fig. 15). For magma derived from ancient crust, its T_{DM} age will be significantly older than its crystallization age.

A hypothetical example of three volcanic rocks, all with the same crystallization age (T_3), is shown in Fig. 15b. The basalt plots on the depleted mantle curve and would be interpreted as a juvenile melt derived directly from the depleted mantle. The rhyolite is highly negative, and following its growth line back to the depleted mantle curve yields a model age of T_1. The rhyolite would be interpreted as being derived from the melting of a continental crustal source that has an average extraction age from the depleted mantle of T_1. The andesite has E_{Nd} values between those of the basalt and the rhyolite, and so cannot be related

by fractionation to either. In this case, a possible interpretation is that the andesite was derived by mixing of basalt and rhyolite. If so, the T_{DM} age of the andesite is merely a happenstance of the mixing process and is therefore geologically meaningless (see Arndt and Goldstein 1987).

As many authors have pointed out, T_{DM} ages can only be used with extreme caution. As magmas ascend to the surface, they may mix or mingle with other melts from different sources, as may be the case in some magma with intermediate compositions. These rocks are actually mixtures of ancient recycled crust and juvenile material extracted from the mantle. Although the range in e_{Nd} values may help deduce the origin of such magmas, the T_{DM} ages have no specific geological meaning (Fig. 15b). However, the tell-tale signs of mixing can generally be detected using field evidence (e.g. presence of xenoliths, evidence of mixing or mingling), microscopic evidence such as textures (e.g. mantled phenocrysts) that indicate disequilibrium, or chemical indicators. Samples contaminated by mixing must be excluded when determining the crustal formation age of the source rocks.

Textural evidence for mixing is commonly found in andesites, including multi-stage growth and oscillatory zoning of plagioclase and pyroxene phenocrysts, the coexistence of olivine and quartz, and the presence of rounded olivine rimmed by pyroxene (e.g. Eichelberger 1975; Eichelberger et al. 2000, 2006; Clynne 1999; see also Murphy 2006).

The influence of source regions on isotopic signatures is classically demonstrated in the Mesozoic–Cenozoic magmatism in western North America. Since the break-up of Pangaea, North America has been moving westward in response to the opening of the Atlantic Ocean. The western margin of North America is on the leading edge of the plate and so it's Mesozoic–Cenozoic history is

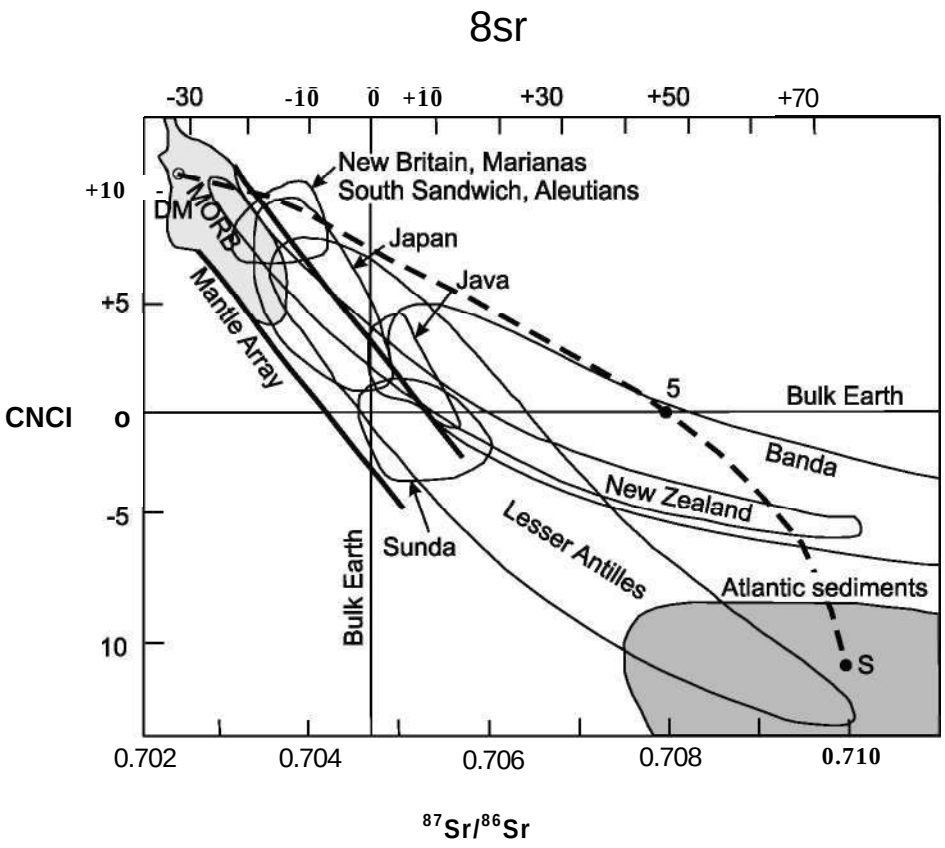

Figure 17. Diagram showing Nd-Sr isotopic variations in modern arc volcanic rocks. Note the negative relationship between $^{87}Sr/^{86}Sr$ and $^{143}Nd/^{144}Nd$ initial ratios (see Gill 1981; Wilson 1989; McCullough 1993; Winter 2001). Although several arc lavas plot near the mantle array, in general the data indicate that there is an additional source other than a depleted mantle component (DM). The data lie on mixing lines between depleted mantle and subducted sediments (e.g. hyperbolic curve [dashed line] between DM and hypothetical sediment composition, S), suggesting that about 5% input from subducted oceanic sediments, or fluids derived from them, may have contributed to the isotopic signature of many arc magmas.

dominated by subduction-related tectonics and collisions of oceanic terranes. Recent studies of terrane accretion in the Canadian Cordillera suggest that some accretionary processes can be "thick-skinned", i.e. up to 100-150 km of lithosphere (MacKenzie et al. 2005). After terrane accretion, subduction zones commonly step outboard, and become re-established along the continental margin (Burchfiel et al. 1992); then, recycling of the mantle roots of the accreted terranes begins (Fig. 17; e.g. Selby et al. 2003).

Armstrong et al. (1977), Kistler and Peterman (1978) and DePaolo (1981a) showed how isotopic signatures of Mesozoic–Cenozoic igneous rocks can constrain the boundary between ancestral North America and the accreted terranes. Magmatism in the accreted terranes has lower (<0.706) $^{87}Sr/^{86}Sr$ initial ratios than that derived from ancestral North America (Armstrong et al. 1977; Kistler and Peterman 1978). In a study of the large batholiths in California and the Sierra Nevada, DePaolo (1981a) showed that $^{87}Sr/^{86}Sr$ initial ratios increase from west to east from 0.703 to 0.708, and together with Sm-Nd isotopes define a west-to-east mixing curve between juvenile magmas with +ve E_{Nd} and crustal magmas with –ve E_{Nd} in the east. These differences are attributed to the more juvenile mantle source for

magmas in the accreted terranes, compared with the ancient source for magmas in ancestral North America.

U-Th-Pb Isotopes

Uranium-Pb isotopic analyses of minerals such as zircon, monazite and titanite are commonly viewed to be the most reliable method available to date igneous and metamorphic events (e.g. Krogh 1973). However, these isotopic systems, in conjunction with Th-Pb systems can also be useful tracers of igneous suites. Uranium, Th and Pb are LIL elements and so are preferentially incorporated in the crustal melts or fluids relative to the mantle during tectonothermal events.

Although the Earth's crust is ultimately derived from the mantle, the chemical exchange is not a one-way street. During subduction, some of the chemical residue from the subducted slab is recycled back into the mantle. Lead ratios indicate that the mantle source of basalts is commonly contaminated by the residue from subducted slabs. Assuming subduction has been active since the Archean, the cumulative effects of this recycling can account for about 10% of the lower mantle composition (Tatsumi 2005). The overall result of this exchange is that the mantle is chemically heterogeneous, and several idealized reservoirs of varying mantle composition have been identified that reflect crust-mantle interactions (Figs. 18, 19). As mantle-derived basalts inherit the isotopic compositions of their source, heterogeneity of the mantle is evident in the subtle, but systematic, variations in the chemical and isotopic composition of basalts from a variety of tectonic settings (Zindler and Hart 1986). The principle source of mantle heterogeneity appears to be related to the descent of subducting slabs into the mantle. Although the exact mechanism is disputed, tomographic imaging of seismic data and geodynamic modelling (Zhong and Gurnis 1997) indicate that subduction zones extend to the core-

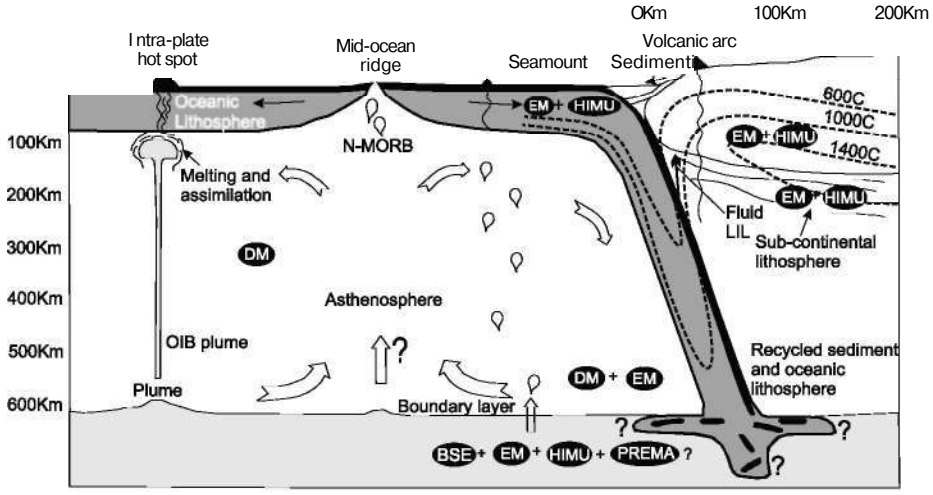

Figure 18. Schematic illustration of the processes that produce mantle heterogeneity. Slabs, carrying sediments, fluids as well as oceanic lithosphere, contaminate the mantle as they penetrate to great depths, resulting in mantle heterogeneity. The mantle has been contaminated with the residue of these slabs since the Archean. This heterogeneity is particularly evident in isotopic studies. Modern-arc systems show the influence of several idealized mantle compositions (see Zindler and Hart 1986), including depleted (DM), prevalent (PREMA), high μ (HIMU) and enriched mantle (EM) (modified from Wilson 1989; Winter 2001).

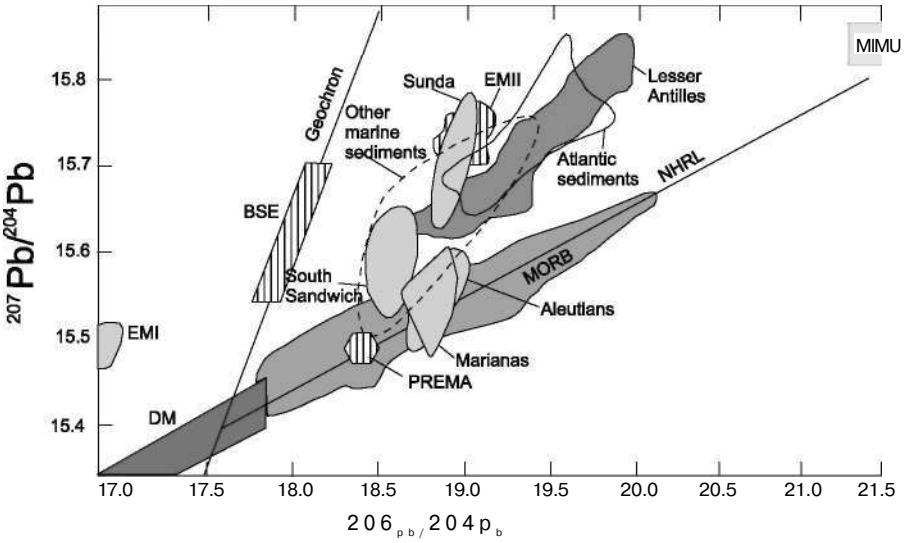

Figure 19. $^{207}Pb/^{204}Pb$ vs 206Pb/204Pb plot showing the fields for several modern arc systems (compiled in Wilson 1989, Winter 2001) and fields for known mantle reservoirs and crustal rocks. All modern suites would plot on the Geochron if their Pb isotopic ratios were unaffected by secondary processes which represents the evolution of undepleted mantle (or BSE, Bulk Silicate Earth). Modern arc systems show the influence of several mantle sources, including depleted (DM), prevalent (PREMA), high [x (HIMU) and enriched (EM-I and EM-II) mantle (Zindler and Hart 1986), a scenario that is consistent with an origin in a metasomatized mantle wedge. NHRL = Northern Hemisphere Reference Line (see Zindler and Hart 1986).

Table 3. Isotopic characteristics of various mantle reservoirs (after Zindler and Hart 1986; Rollinson 1993; Winter 2001). DM = depleted mantle, PREMA = prevalent mantle, HIMU = high μ mantle. DM is the probable source of mid-ocean ridge basalt. PREMA is a dominant reservoir of oceanic island rocks (see Greenough et al. 2005). HIMU is highly radiogenic mantle, its high $^{206}Pb/^{204}Pb$ indicating a source rich in U. EM-I and EM-II are two types of enriched mantle. EM-I may represent a mantle contaminated with recycled oceanic or lower continental crust. EM-II may represent a mantle contaminated with upper continental crust (or sediments derived from upper continental crust).

	$^{87}Sr/^{86}Sr$	143Nd/144Nd	206Pb/204Pb	207Pb/204Pb
Bulk Earth	0.7052	0.51264	18.4	15.58
DM	0.7015-0.7025	0.5133-0.5136	15.5-17.7	<15.45
PREMA	0.7033	<0.5128	18.2-18.5	15.4-15.5
HIMU	0.7025-0.7035	0.511-0.5121	21.2-21.7	15.8-15.9
EM-I	c. 0.705	<0.5112	17.6-17.7	15.46-15.49
EM-II	>0.722	0.511-0.512	16.3-17.3	15.4-15.5
Upper Crust	0.72-0.74	0.507-0.513	up to 28	up to 20

mantle boundary and contribute to convection systems in the mantle. The isotopic data suggest that these subduction zones deliver refractory components to the mantle which are derived from oceanic sediments and lithosphere that were not extracted and incorporated into the overlying mantle wedge. This interaction happens continuously as subduction proceeds, but it can also occur when the slab breaks and founders into the mantle during collisional orogenesis (Whalen et al. 1996; Hildebrand and Bowring 1999), or potentially during slab avalanche events (Tan et al. 2002).

From studying the Pb isotopic characteristics of terrestrial basalts, there is a consensus among petrologists that at least five isotopically distinct reservoirs exist in the mantle. For example, the ocean island basalts of St. Helena are highly enriched in $^{206}Pb/^{204}Pb$ and $^{207}Pb/^{204}Pb$ relative to DM, and characterize an isotopic reservoir known as HIMU (high (X). The isotopic characteristics of these reservoirs are shown in Table 3 (after Rollinson 1993).

The $^{207}Pb/^{204}Pb$ vs $^{206}Pb/^{204}Pb$ plot (Fig. 19) is particularly instructive. The data from a given suite are compared to the known values of potential mantle reservoir and crustal rocks, and to the "geochron", which is a line where all data from modern suites plot if their Pb isotopic compositions are unaffected by secondary processes. A hypothetical un-depleted mantle (known as BSE, Bulk Silicate Earth), also plots on this line because such a mantle, by definition, is not affected by events that would have fractionated U, Pb or Th into the crust.

Despite a broad consensus on their existence, the origin of some of the reservoirs in Table 3 is controversial. The reservoir that is most commonly represented at the surface is the depleted mantle (DM), the mantle from which basalt has been extracted during seafloor spreading. Mid-ocean ridge basalts lie close to DM but clearly contain another isotopic component. As subduction zones recycle MORB and the underlying DM, it is not surprising that many arc basalts have a similar Pb isotopic signature to MORB. Like MORB, Pb isotopes indicate that arc magmas have an important (but not exclusive) DM component, an interpretation consistent with trace element and Sm-Nd isotopic data discussed above.

Many petrologists, including Greenough et al. (2005), have drawn attention to the fact that data from arc magmas are either spread along or above the join between DM and HIMU (Fig. 19). Those that plot along the DM-HIMU join (e.g. Aleutians) can be explained by contributions from both reservoirs, and the data that plot above the line (e.g. South Sandwich, Sunda, Lesser Antilles) require the additional influence of a third reservoir, possibly EM-II, which is thought to reflect contamination of the mantle by dehydrated subducted sediments (e.g. Johnson and Plank 1999).

The origin of HIMU is controversial. Its strong radiogenic lead enrichment suggests a source that is enriched in U relative to Pb (Chauvel et al. 1992). Tatsumi and Kogiso (2003) point out that the residue of dehydrated MORB would be relatively enriched in U, and would, over time yield high $^{206}Pb/^{204}Pb$ and $^{207}Pb/^{204}Pb$ values, because MORB loses Pb as it dehydrates in a subduction zone. If so, the Pb-isotopic signal of arc basalts could be derived from a mantle source that has previously assimilated ancient oceanic crust, presumably the residue of ancient subducted slabs.

In summary, U-Pb isotopes from basaltic rocks indicate that the mantle source for modern arc magmas reflects contamination by hundreds of millions, if not billions, of years of subduction. It is clear that arc magmas are influenced by several isotopic reservoirs. These reservoirs share a fundamental property: their Pb-isotopic compositions are too enriched in Pb to be explained by internal mantle processes. The cumulative effects of contamination from the residues of ancient subduction zones are required to explain them.

OTHER ARC ROCKS

Not all magmas generated in arc environments fit neatly into calc-alkalic, tholeiitic or alkalic classifications. Shoshonites, boninites and adakites are volumetrically small, but are nonetheless petrologically significant igneous rocks that form in specialized arc environments. Their occurrence reveals

much about the thermal structure of the arc and the potential effects of some complications induced by local tectonic activity.

Shoshonite is an alkali-rich (Na_2O+K_2O > 6.5 wt %) trachyandesite that occurs in continental rift, collisional and arc settings (Rogers and Setterfield 1994). Shoshonite occurs in association with calc–alkaline volcanism in intra-arc rift settings, in intra-oceanic island arcs and backarc basins, (Sun and Stern 2001; Adams et al. 2005) and continental arcs (Conrey et al. 1997). In oceanic arcs, shoshonite magma development is related to a change in subduction processes or arc-rifting (Rogers and Setterfield 1994). In continental arcs, shoshonite generally occurs a significant distance from the trench where the subducted slab is at a great depth and is commonly associated with rifting of the arc or backarc (Gill 1981; Baluyev et al. 1988). Shoshonites in all environments are markedly enriched in LIL (100-1000× chondrite), including LREE. The high Ce/Yb is attributed to LREE enrichment, and the role of residual garnet in the source. The subduction component in shoshonites is also indicated by pronounced negative Nb, Ti and Ta anomalies (e.g. Turner et al. 1996).

Boninites (named after the Bonin Islands, south of Japan, where they are most abundant, Cameron et al. 1979, 1983) are high MgO (> 6 wt% MgO) andesites that predominantly occur in the early stages of oceanic arc development in fore-arc regions, an unusual locality for magma generation. Compared to typical andesites, they have higher Cr, Ni and LIL elements but lower Ti and Nb (Arndt 2003). They are generally thought to represent melting of a hydrated and refractory Mg-rich mantle wedge that was contaminated with LIL elements transported from the subduction zone. It is clear that to generate boninitic magma, a steep geothermal gradient is needed to melt depleted peridotite. Such environments can occur in some extensional environments within the arc, either at shallow levels in the fore-arc, or where a backarc spreading centre propagates into an active arc. Published models for the origin of boninites include 1) the initiation of subduction (Stern and Bloomer 1992), 2) intra-arc rifting (Crawford et al. 1981; 3) ridge subduction (Cameron 1989), 4) the effect of seafloor spreading in a forearc basin (Bedard et al. 1998) or 5) where an active arc undergoes backarc spreading (e.g. Falloon and Crawford 1991; Monzier et al. 1993).

Adakites (Kay 1978; Defant and Drummond 1990; Defant and Kepezhinskas 2001; Grove et al. 2005), named after Adak Island in the Aleutians, are also high-Mg andesites, but unlike boninites, they are very LREE enriched (normalized La/Yb > 40), contain high Sr (> 400 ppm), high Sr/Y values, low initial $^{87}Sr/^{86}Sr$ and low ratios of radiogenic to non-radiogenic Pb. Kay (1978) attributed adakites to the interaction of a LIL element-rich hydrous melt from the subducted oceanic crust with overlying mantle, and then eruption without interaction with the island arc crust. The question then becomes: under what conditions does the slab become hot enough to melt? Models favouring the subduction of young crust (e.g. Green and Harry 1999) are supported by experiments where adakites are produced by reaction of slab melts with peridotite in the mantle wedge (e.g. Rapp et al. 1999). The thermal structure of subduction zones (e.g. Peacock et al. 1994) predicts that only very young oceanic crust (<5 Ma) can melt. This prediction is at odds with geologic data (e.g. Defant and Drummond 1990) which indicate that slab melting occurs in crust as old as 20 Ma. This discrepancy is attributed to a higher contribution from shear heating in subduction zones than is accounted for in the Peacock et al. model (Green and Harry 1999). Dickinson and Snyder (1979) and Thorkelson (1996) show that in a ridge-trench collisional environment, a "window" in the slab forms between the downgoing plates that is filled with upwelling asthenosphere. Such an environment can induce slab melting along the thinned margins of the window (Johnston and Thorkelson 1997; Thorkelson and Breitsprecher 2005). Defant and Kepezhinskas (2001) propose that slab melting and adakite production can also occur near tears in the subducted slab, which also facilitates asthenospheric upwelling. It is clear that slab melting may occur in several environments, but the common denominator appears to be anomalous local supply of heat.

Adakites have recently been recognized in many other localities in the modern and ancient record. Indeed, some authors use them as an analogy for generating Archean magmas, in which it is viewed that the more elevated geothermal gradient might result in more common melting of the slab (Martin et al. 2005). Archean complexes are dominated by trondhjemite, tonalite and granodiorite (the so called TTG suite, Martin 1987). During the Archean, it is generally believed that the geothermal gradient was higher implying a hotter upper mantle than today (e.g. de Wit and Hynes 1995) which could promote slab melting (e.g. Martin 1987; Defant and Drummond 1990). Experiments suggest that slabs under these conditions can melt, and if that melt interacts with the mantle, it can produce intermediate compositions similar to those of Archean complexes (Rapp et al. 1999; Tatsumi 2000).

DISCUSSION

There are several possible sources for arc magmas in the vicinity of the subduction zone, including the subducted oceanic crust and sediments, as well as the mantle wedge and crust above the subduction zone.

To a greater or lesser extent, a

chemical signal from all these sources can be found in arc magmas. However, when the thermal conditions in the vicinity of the subduction zone are considered in conjunction with phase equilibria, it is clear that arc magmas are most commonly generated in the mantle wedge and crust above the subduction zone. The thermal regime at subduction zones is profoundly influenced by the rate of descent of cold oceanic lithosphere, which is generally too fast to allow significant transfer of heat from the surrounding mantle. As a result, the isotherms are deflected downwards, and this cooling leads to a low geothermal gradient (10-15°C per km) and low heat flow in the fore-arc region above the subducted slab. As it descends, the slab is slowly warmed up, so that sediments, oceanic crust and lithosphere undergo prograde blueschist-eclogite facies metamorphism resulting in dehydration of the slab.

Although magma is not produced, the subducted oceanic lithosphere does play a vital role in the origin of arc magmas because the metamorphic fluids are released and migrate upward to invade and chemically modify the overlying mantle wedge. Of all the magmas formed in a subduction zone environment, IATs show the least contamination from subduction zone processes, an interpretation consistent with their occurrence in immature arcs. In more mature arcs, the effect of the fluids is more profound. The hydrated mantle melts at a significantly lower temperature than dry mantle and the magmas produced are oxidized and hydrated, inducing early crystallization of minerals such as magnetite and hornblende, which inhibit the rise in Fe/Mg ratio and so produce a calc-alkalic trend.

These oxidizing fluids tend to be enriched in water-soluble LIL elements. They also may stabilize HFS-bearing accessory minerals so that magmas derived from the mantle wedge tend to be enriched in LIL but depleted in HFS elements, patterns that are clearly evident in MORB-normalized or mantle-normalized spidergram plots in which HFS depletion is identified by negative Nb and Ti anomalies.

Except in rare cases, the subducted oceanic lithosphere does not attain temperatures that are sufficient for it to melt, so that the slab itself cannot be the main source of arc magmas. Relatively flat HREE profiles for most arc magmas are consistent with a derivation from the spinel lherzolite portion (< 50 km depth) of the mantle. For similar reasons, the asthenospheric mantle below the slab does not warm up appreciably and so cannot be an important source of magma. Adakites, however, which do show significant HREE depletion, may well be representative of slab melts, but they are rare, and their formation requires anomalous local supplies of heat within the subduction regime.

The Sr, Nd and Pb isotopic signatures of continental arc magmas commonly have a crustal component. In some arcs, these signatures are imposed by crustal contamination as the magma rises toward the surface. However, other arcs have this signature, even if they are capped by oceanic, rather than continental crust. The only plausible sedimentary source is from the subduction zone itself, supporting the notion that sediments are dragged down the subduction zone, and LIL elements derived from them are introduced into the mantle wedge. This hypothesis is supported by elevated concentrations of boron and beryllium in arc volcanic rocks, which can only be derived from subduction of recent sediments (e.g. Morris et al. 1990).

In mature subduction zones, original chemistry of the mantle wedge is progressively blurred by metasomatic fluids from the subducting slab. Depending on previous history, the mantle wedge may have a quite variable initial chemistry, which can influence the compositions of early arc magmas.

As arc magmas rise toward the surface, their compositions are strongly modified by interaction with their surroundings, especially during final cooling. Intermediate to silicic arc magmas can form in a variety of ways, including fractional crystallization of a more mafic parent, mixing between mafic and felsic magmas, partial melting of the crust, and assimilation and digestion of the crust by more mafic magma. Where felsic magmas are voluminous relative to intermediate or mafic melts, they are unlikely to be generated by fractional crystallization because there is not enough parent mafic magma to produce the felsic differentiates. Andesites formed either by mixing of basaltic and rhyolitic magmas, or by contamination of a more mafic parent by the continental crust commonly display textural evidence of disequilibrium (Eichelberger 1975) or field evidence of magma mixing or host rock assimilation (Wiebe et al. 2002). All these processes seem to occur in arc magmas to some extent although their relative importance may vary from one suite to another, or even within a given suite.

The extent of crustal involvement in the composition of intermediate to felsic magmas can be assessed using isotopes. Samarium-Nd isotopes are particularly robust because they are normally not affected by secondary processes. Magmas related by fractional crystallization should yield similar Sm-Nd isotopic signatures. Those formed by anatexis of older crust should have depleted mantle model ages that are significantly older than their crystallization age and those that reflect contamination or assimilation should plot on calculated mixing curves and should have a range in T_{DM} ages between the end member components (DePaolo 1981a, b; Arndt and Goldstein 1987).

Given that 1) intermediate rocks are the dominant product of arc

magmatism, and 2) they approximate the average composition of the continental crust, identifying the dominant process that forms intermediate magmas is fundamental to the understanding of crustal evolution.

Although hotly debated (e.g. Hamilton 1998; Stern 2005), many geologists contend that arcs have existed at least since the end of the Archean. Much of the petrological evidence is derived from geochemical and isotopic studies, which indicate that Late Archean volcanic and plutonic rocks share many similar geochemical traits with their modern counterparts (see Dostal and Mueller 1997; Corcoran and Dostal 2001; Canil 2004; Cousens et al. 2004; Dostal et al., 2004). If so, then processes like those occurring in modern arcs may well have had an influence on the evolution of continental crust for at least the last 2.5 billion years.

ACKNOWLEDGEMENTS

Much of what I have learned about arc magmatism has been through collaboration and conversations with colleagues including Alan Anderson, Randy Cormier, Richard D'Lemos, Jarda Dostal, Javier Fernandez-Suarez, Gabi Gutierrez-Alonso, Andrew Hynes, Duncan Keppie, Damian Nance, Georgia Pe-Piper, Cecilio Quesada, Rob Strachan and participants in various UNESCO-IGCP projects. I am grateful to NSERC Canada for research funding, for which arc systems are a major part, to Derek Thorkelson, and Stephen Johnston for thorough, constructive reviews, Sonya Dehler, Steve McCutcheon and Georgia Pe-Piper for editorial advice, and Matt Middleton for cheerful technical assistance.

REFERENCES

Adams, M.G., Lentz, D.R., Shaw, C.S.J., Williams, P.F. Archibald, D.A. and Cousens, B., 2005, Eocene shoshonitic mafic dykes intruding the Monashee Complex, British Columbia: a petrogenetic relationship with the Kamloops Group volcanic sequence?: Canadian Journal of Earth Sciences, v. 42, p. 11-24

Arculus, R.J., and Curran, E.B., 1972, The genesis of the calc-alkaline rock suite: Earth and Planetary Science Letters, v. 15, p. 255-262.

Allegre, C.J., Treuil, M., Minster, J.F., Minster, J.B., and Albarebe, F., 1977, Systematic use of trace elements in igneous processes. I Fractional crystallization in volcanic suites: Contributions to Mineralogy and Petrology, v. 60, p. 57-75.

Armstrong, R.L., Taubeneck, W.H., and Hales, P.O., 1977, Rb-Sr and K-Ar geochronometry of Mesozoic granitic rocks and their Sr isotopic composition, Oregon, Washington, and Idaho: Geological Society of America Bulletin, v. 88, p. 397-411.

Arndt, N.T., 2003, Komatiites, kimberlites and boninites: Journal of Geophysical Research, v. 108, p. B6, 229.

Arndt, N.T. and Goldstein, S.L., 1987, Use and abuse of crust formation ages: Geology, v. 15, p. 893-895.

Baluyev, E.Y., and Perepelov, A.B., 1988, Mineralogical and geochemical features of high-potash andesites in the frontal part of the Kamchatka island arc: Geokhimiya, v. 6, p. 813-824.

Bedard, J. H., Lauziere, K., Tremblay, A., and Sangster, A., 1998, Evidence for forearc seafloor-spreading from the Betts Cove ophiolite, Newfoundland: oceanic crust of boninitic affinity: Tectonophysics, v. 284, p. 233-245.

Blatt, H., Tracy, R.J., and Owens, B., 2005, Petrology, Igneous, Sedimentary, Metamorphic, 3rd Edition: W.H. Freeman Publishers, 529 p.

Boettcher, A.L., 1977, The role of amphibole and water in circum-Pacific volcanism, *in* Manghnani, M.H. and Akimoto, S., *eds.*, High Pressure Research Applications in Geophysics. Academic Press, London, p.107-126.

Boudreau and McBirney, A.R., 1997, The Skaergaard Layered Series. Part III. Non-dynamic layering: Journal of Petrology, v. 38, p.1003-1020.

Burchfiel, B.C., Lipman, P.W., and Zoback, M.L., *eds*, 1992, The Cordilleran Orogen: conterminous U.S.:, v. G-3, Geological Society of America, Boulder, Colorado, 724p.

Cameron, W.E., 1989, Contrasting boninite-tholeiite associations from New Caledonia, *in* Crawford, A.J., *ed*., Boninites: Unwin-Hyman, London, p. 314-338.

Cameron, W. E., Nisbet, E. G., and Dietrich, V. J., 1979, Boninites, komatiites and ophiolitic basalts: Nature, v. 280, p. 550-553.

Cameron, W. E., McCulloch, M. T., and Walker, D. A., 1983, Boninite petrogenesis: chemical and Nd-Sr isotopic constraints: Earth and Planetary Science Letters, v. 65, p. 75-89.

Canil, D., 2004, Mildly incompatible elements in peridotite and the origins of mantle lithosphere: Lithos, v. 77, p. 375-393.

Carmichael, I.S., 2002, The andesite aqueduct: perspectives on the evolution of intermediate magmatism in west-central (105-99°W) Mexico: Contributions to Mineralogy and Petrology, v. 143, p. 641-663.

Chauvel, C., Hofmann, A.W., and Vidal, P., 1992, HIMU-EM: The French Polynesian connection: Earth and Planetary Science Letters, v. 110, p. 99-119.

Clynne, M.A., 1999, A complex magma mixing origin for rocks erupted in 1915, Lassen peak, California: Journal of Petrology, v. 40, p. 105-132.

Collins, W.J., 2002, Hot orogens, tectonic switching and creation of continental crust: Geology, v. 31, p. 535-538.

Condie, K.C., 1989, Geochemical changes in basalts and andesites across the Archean–Proterozoic boundary: identification and significance: Lithos, v. 23, p. 1-18.

Conrey, R.M., Sherrod, D.R. Hooper, P.R and Swanson, D.A., 1997, Diverse primitive magmas in the Cascade arc, northern Oregon and southern Washington: Canadian Mineralogist, v. 35, p. 367-396.

Corcoran, P. L. and Dostal, J. 2001, Development of an ancient back-arc basin overlying continental crust: the Archean Peltier Formation, Northwest Territories, Canada: Journal of Geology, v. 109, p. 329-348.

Cousens, B.L., Aspler, L.B., and Chiarenzelli, J.R., 2004, Dual sources of ensimatic Neoarchean magmas, and infant-arc processes, Henik segment, Hearne domain, western Churchill

Province, Nunavut, Canada: Precambrian Research, v. 134, p. 169-188.

Cox, K.G., Bell, J.S., and Pankhurst, R.J., 1979, The Interpretation of Igneous Rocks: Allen and Unwin, London, 450 p.

Crawford, A. J., Beccaluva, L., and Serri, G., 1981, Tectono-magmatic evolution of the West Philippine-Mariana region and the origin of boninites: Earth and Planetary Science Letters, v. 54, p. 346-356.

Defant, M.J., and Drummond, M.S., 1990, Derivation of some modern arc magmas by melting of young subducted lithosphere: Nature, v. 347, p. 662-665.

Defant, M.J., and Kepezhinskas, P., 2001, Evidence suggests slab melting in arc magmas: EOS Transactions, v. 82, p. 65-69.

DePaolo, D.J., 1981a, A neodymium and strontium isotopic study of the Mesozoic calc-alkaline granitic batholiths of the Sierra Nevada and Peninsula ranges: Journal of Geophysical Research, v. 86, B11, p. 10470-10488.

DePaolo, D.J., 1981b, Neodymium isotopes in the Colorado Front Range and crust-mantle evolution in the Proterozoic: Nature, v. 291, p. 193-196.

DePaolo, D.J., 1988, Neodymium Isotope Geochemistry: An Introduction: Springer Verlag, New York, 187p.

Dewey, J.F., 1980, Episodicity, sequence and style at convergent plate margins: Geological Association of Canada, Special Paper 20, p. 553-574.

de Wit, M.D., and Hynes, A., 1995, On the onset of hydrothermal cooling of Earth and the origin of its first continental lithosphere: Geological Society of London, Special Publication 95, p. 1-9.

Dickinson, W.R., 1975, Potash-depth (K-h) relations in continental margins and intra-oceanic magmatic arcs: Geology, v. 3, p. 53-56.

Dickinson, W.R., and Snyder, W.S., 1979, Geometry of subducted slabs related to the San Andreas transform: Journal of Geology, v. 87, p. 609-627.

Dostal, J. and Mueller, W.U., 1997, Komatiite flooding of a rifted Archean rhyolitic arc complex: Geochemical signature and tectonic significance of the Stoughton-Roquemaure Group, Abitibi greenstone belt, Canada: Journal of Geology, v. 105, p. 545-563.

Dostal, J., Mueller, W.U. and Murphy, J.B., 2004, Archean molasse basin evolution and magmatism, Wabigoon Subprovince, Canada: Journal of Geology, v. 112, p. 435-454.

Eggler, D.C., 1978, The effect of CO_2 on the partial melting of peridote in the system Na_2O-CaO-Al_2O_3-MgO-SiO_2-CO_2 to 35 kb, with analysis of melting in a peridotite-H_2O- CO_2 system: American Journal of Science, v. 278, p. 305-343.

Eichelberger, J.C., 1975, Origin of andesite and dacite; evidence of mixing in Glass Mountain in California and at other circum-Pacific volcanoes: Geological Society of America Bulletin, v. 86, p. 1381-1391.

Eichelberger, J.C., Chertkoff, D.G., Dreher, S.T., and Nye, C.J., 2000, Magma in collision: rethinking chemical zonation in magma chambers: Geology, v. 28, p. 603-628.

Eichelberger, J.C., Izbekov, P.E., and Browne, B.L. 2006, Bulk chemical trends at arc volcanoes are not liquid lines of descent: Lithos, v. 87, p. 135-154.

Falloon, T.J., and Crawford, A.J., 1991, The petrogenesis of high-calcium boninite lavas dredged from the northern Tonga ridge: Earth and Planetary Science Letters, v. 102, p. 375-394.

Faure, G., 1997, Principles of Isotope Geology: John Wiley & Sons, New York.

Faure, G., and Mensing, T.M., 2005, Isotopes: Principles and Applications, 3rd Edition, 897 p

Gill, J.B., 1981, Orogenic Andesites and Plate Tectonics: Berlin, Springer Verlag, 390 p.

Ghioso, M.S., and Sack, R.O., 1995, Chemical mass transfer in magmatic processes IV. A revised and internally consistent thermodynamic model for the interpolation and extrapolation of liquid-solid equilibria in magmatic systems at elevated temperatures and pressures: Contributions to Mineralogy and Petrology, # 119, p. 197-212.

Green, N.L., and Harry, D.L, 1999, On the relationship between subducted slab age and arc basalt petrogenesis, Cascadia subduction system, North America: Earth and Planetary Science Letters, v. 171, p. 367-381.

Greenough, J.D, Dostal, J., and Mallory-Greenough, L.M., 2005, Ocean Island Volcanism II: Mantle Processes: Geoscience Canada, v. 32, no.2, p. 77-90.

Grove, T.L., and Baker, M.B., 1984, Phase equilibrium controls on the tholeiitic versus calc-alkaline differentiation trends: Journal of Geophysical Research, v. 89, p. 3253-3274.

Grove, T.L., Elkins-Tanton, L.T., Parman, S.W., Chatterjee, N., Müntener, O., and Gaetani, G.A., 2003, Fractional crystallization and mantle-melting controls on calc-alkaline differentiation trends**:** Contributions to Mineralogy and Petrology, v. 145, p. 515-533.

Grove, T. L., Baker, M.B., and Price, R.C., Parman, S.W., Elkins-Tanton, L.T., Chatterjee, N., and Müntener, O., 2005, Magnesian andesite and dacite lavas from Mt. Shasta, northern California: products of fractional crystallization of H_2O-rich mantle melts: Contributions to Mineralogy and Petrology, v. 148, p. 542-565.

Hamilton, W.B., 1998, Archean magmatism and deformation were not products of plate tectonics: Precambrian Research, v. 91, p. 143-179.

Hanson, G.N., 1978, The application of trace elements to the petrogenesis of igneous rocks of granitic composition: Earth and Planetary Science Letters, v. 38, p. 26-43.

Hildebrand, R.S., and Bowring, S.A., 1999, Crustal recycling by slab failure: Geology, v. 27, p. 11-14.

Hynes, A., 1980, Carbonatization and mobility of Ti, Y and Zr in Ascot Formation metabasalts, SE Quebec: Contributions to Mineralogy and Petrology, v. 75, p. 79-87.

Irvine, T.N., and Baragar, W.R.A., 1971, A guide to the chemical classification of the common volcanic rocks: Canadian Journal of Earth Sciences, v. 8, p. 523-548.

Johnson, M.C., and Plank, T., 1999, Dehydration and melting experiments constrain the fate of subducted sediments: Geochemistry, Geophysics, Geosystems, v. 1, doi: 10:1029/1999GC000014.

Johnston, S.T., and Thorkelson, D.J., 1997, Cocos-Nazca slab window beneath central America: Earth and Planetary Science Letters, v. 146, p. 465-474.

Kay, R.W., 1978, Aleutian magnesian andesites: melts from subducted Pacific Ocean crust: Journal of Volcanology and Geothermal Research v. 4, p. 117-132.

Kelemen, P.B., 2004, One view of the geochemistry of subduction-related magmatic arcs, with an emphasis on primitive andesite and lower crust, *in* Treatise on Geochemistry, *eds*., H.D. Holland and K.K. Turekian. Elsevier-Pergamon, Oxford, p. 593-659.

Kistler, R.W., and Pererman, Z.E., 1978, Reconstruction of crustal blocks of California on the basis of strontium initial compositions of Mesozoic granitic rocks: United States Geological Survey Professional Paper 1071, 17p.

Krogh, T.E., 1973, A low contamination method for the hydrothermal decomposition of zircon and extraction of U and Pb for isotopic age determinations: Geochimica et Cosmochimica Acta, v. 37, p. 485-494.

Kuno, H., 1966, Lateral variation of basaltic magma type across continental margins and island arcs: Bulletin of Volcanology, v. 29, p. 195-222.

Langmuir, C.H., Vocke, R.D., Hanson, G.N., and Hart, S.R., 1978, A general mixing equation with application to Icelandic basalts: Earth and Planetary Science Letters, v. 37, p. 380-392.

Lee, C.-T.A., Leeman, W.P., Canil, D., and Li, Z-X. A., 2005**,** Similar V/Sc systematics in MORB and arc basalts: Implications for the oxygen fugacities of their mantle source regions: Journal of Petrology, v. 46, p. 2313-2336.

LeMaitre, R.W., *ed*.; Bateman, P., Dudek, A., Keller, J., Lemeyre, J., Le Bas, M.J., Sabine, P.A., Schmid, R., Sorensen, H., Steckeisen, A., Wooley, A.R., and Zanettin, B., 1989, A Classification of Igneous Rocks and a Glossary of Terms: Blackwell Scientific, Oxford, United Kingdom, 193p.

Leterrier, J., Maury, R.C., Thonon, P., Girard, D., and Marchal, M., 1982, Clinopyroxene composition as a method of identification of the magmatic affinities of paleo-volcanic series: Earth and Planetary Science Letters, v. 59, p. 139-154.

Liebscher, A., 2004, Discussion: Decoupling of fluid and trace element release in subducting slab? Comment on Redistribution of trace elements during prograde metamorphism from lawsonite blueschist to eclogite facies; implications for deep subduction-zone processes by C. Spandler et al. (Contributions to Mineralogy and Petrology, v. 146, p. 205-222, 2003): Contributions to Mineralogy and Petrology, v. 148, p. 502-505.

MacDonald, G.A, 1968, Composition and origin of Hawaiian lavas, *in* Coats, R.R. Hay, R.L., and Anderson, C.A., *eds*., Studies in Volcanology; a Memoir in honor of Howel Williams: Geological Society of America Memoir 116.

MacKenzie, J.M., Canil, D., Johnston, S.T., English, J., Mihalynuk, M.G., and Grant, B., 2005, First evidence for ultrahigh-pressure garnet peridotite in the North American Cordillera: Geology, v. 33, p. 105-108.

Martin, H., 1987, Petrogenesis of Archean Trondhjemites, tonalities and granodiorites from eastern Finland: Journal of Petrology, v. 28, p. 921-953.

Martin, H., Smithies, R.H., Rapp, R., Moyen J.-F. and Champion, D., 2005, An overview of adakite, tonalite–trondhjemite–granodiorite (TTG), and sanukitoid: relationships and some implications for crustal evolution: Lithos, v. 79, p. 1-24.

McCulloch, M.T, 1993, The role of subducted slabs in an evolving Earth**:** Earth and Planetary Science Letters, v. 115, p. 89-100.

McCulloch, M.T. and Gamble, J.A., 1991, Geochemical and geodynamical constraints on subduction zone magmatism: Earth and Planetary Science Letters, v. 102, p. 358-374.

McCulloch, M.T. and Gamble, J.A., 1991, Geochemical and geodynamical constraints on subduction zone magmatism: Earth and Planetary Science Letters, v. 102, p. 358-374.

Miller, C.F., and Mittlefehldt, D.W., 1982, Depletion of light rare-earth elements in felsic magmas: Geology, v. 10, p. 129-133.

Miškovic[!], A., and Francis, D., 2006, Interaction between mantle-derived and crustal calc-alkaline magmas in the petrogenesis of the Paleocene Sifton Range volcanic complex, Yukon, Canada: Lithos, v. 71, p. 135-152.

Miyashiro, A., 1974, Volcanic rock series in island arcs and active continental margin: American Journal of Science, v. 274, p. 321-355.

Monzier, M., Danyushevsky, L.V., Crawford, A.J., Bellon, H., and Cotton, J., 1993, High Mg-andesites from the southern termination of the New Hebrides island arc (SW Pacific): Journal of Volcanology and Geothermal Research, v. 57, p. 193-217.

Morris, J.D., Leeman, W.P., and Tera, F., 1990, The subducted component in island arc lavas: evidence from Be isotopes and B-Be systematics: Nature, v. 344, p. 31-36.

Morris, J.D., and Ryan, J.G, 2004, Subduction zone processes and implications for changing composition of the upper and lower mantle, *in* Treatise on Geochemistry, *ed.*, H.D. Holland and K.K. Turekian, Elsevier-Pergamon, Oxford, p. 451-470.

Murphy, J.B., 2006, Arc Magmatism I: Relationship between tectonic evolution and petrogenesis: Geoscience Canada, v. 33, no. 4, p.145-167

Murphy, J.B., Keppie, J.D., Dostal, J., and Cousens, B.L., 1996, Repeated lower crustal melting beneath the Antigonish Highlands, Avalon Composite Terrane, Nova Scotia: Nd isotopic evidence and tectonic implications, *in* Nance, R.D., and Thompson, M.D., *eds.*, Avalonian and related peri-Gondwanan terranes of the circum North Atlantic: Geological Society of America Special Paper 304, p. 109-120.

Mysen, B.O., 1988, Structure and Properties of Silicate Melts: Elsevier, Amsterdam.

Mysen, B.O. and Boettcher, A.L., 1975, Melting of a hydrous mantle. I. Phase relations of natural peridotite at high pressures and temperatures with controlled activities of water, carbon dioxide and hydrogen: Journal of Petrology, v. 33, p. 347-375.

Peacock, S.M., Rushmer, T., and Thompson, A.B., 1994, Partial melting of subducting oceanic crust: Earth and Planetary Science Letters, v. 121, p. 227-244.

Pearce, J.A., 1982, Trace element characteristics of lavas from destructive plate boundaries, *in* Thorpe, R.S., *ed*., Andesites. Wylie and Sons, p. 525-548.

Pearce, J.A., 1996, A user's guide to basaltic discrimination diagrams, *in* Wyman, D.A., *ed.*, Trace element geo-

chemistry of volcanic rocks: applications for massive sulphide exploration: Geological Association of Canada Short Course Notes, v. 12, p. 79-113.

Pearce, J.A., and Cann, J.R., 1973, Tectonic setting of basic volcanic rocks using trace element analyses: Earth and Planetary Science Letters, v. 19, p. 290-300.

Pearce, J.A., and Norry, M.J., 1979, Petrogenetic implications of Ti, Zr, Y and Nb variations in volcanic rocks: Contributions to Mineralogy and Petrology, v. 69, p. 33-47.

Pearce, J.A., Alabaster, T., Shelton, A.W., and Dearle, M.P., 1981, The Oman ophiolite as a Cretaceous arc-basin: evidence and implications: Philosophical Transactions of the Royal Society of London, v. A300, p. 299-317.

Pearce, J.A., Harris, N.B.W., and Tindle, A.G., 1984, Trace element discrimination diagrams for the tectonic interpretation of granitic rocks: Journal of Petrology, v. 25, p. 956-983.

Rapp, R.P., Shimizu, N., Norman M.D., and Applegate, G.S., 1999, Reaction between slab-derived melts and peridotite in the mantle wedge; experimental constraints at 3.8 GPa: Chemical Geology, v. 160, p. 335-356.

Ringwood, A.E., 1977, Petrogenesis in island arc systems, *in* Talwani, M., and Pitman, W.C., *eds*., Island Arcs, Deep Sea Trenches and Back-arc basins. Maurice Ewing Series #1, American Geophysical Union, Washington, D.C., p. 311-324.

Rollinson, H.R., 1993, Using Geochemical Data: Evaluation, Presentation, Interpretation: Longman/Wyllie, Harlow/New York.

Rogers, N., and Setterfield, T., 1994, Potassium and incompatible-element enrichment in shoshonite lavas from the Tavua volcano, Fiji: Chemical Geology, v. 118, p. 43-62.

Saunders, A.D., and Tarney, J., 1984, Geochemical characteristics of basaltic volcanism in back-arc basins, *in* Kokelaar, B.P., and Howells, M.F., *eds*., Marginal Basin Geology: Volcanic and Associated Sedimentary and Tectonic Processes in Modern and Ancient Marginal Basins: Geological Society of London, Special Publication 16, p. 59-76.

Saunders, A.D., Norry, M.J., and Tarney, J., 1991, Fluid influence on the trace element composition of subduction zone magmas: Philosophical Transactions of the Royal Society of London, v. 335, p. 377-392.

Selby, D, Creaser, R.A., Heaman, L.M, and Hart, C.J.R., 2003, Re-Os and U-Pb geochronology of the Clear Creek, Dublin Gulch and Mactung deposits, Tombstone Creek, Yukon: absolute timing relationships between plutonism and mineralization: Canadian Journal of Earth Sciences, v. 40, p. 1839-1852.

Shaw, D.M. 1970, Trace element fractionation during anatexis: Geochimica et Cosmochimica Acta, v. 34, p. 237-243.

Shelley, D., 1993, Igneous and Metamorphic Rocks under the Microscope: Chapman and Hall, London.

Sisson, T.W., and Grove, T.L., 1993, Experimental investigations of the role of H_2O in calc-alkaline differentiation and subduction zone magmatism: Contributions to Mineralogy and Petrology, v. 113, p. 143-166.

Sisson, T.W., Ratajeski,K., Hankins,W.B., and Glazner, A.F., 2005, Voluminous granitic magmas from common basaltic sources: Contributions to Mineralogy and Petrology, v. 148, p. 635-661.

Spandler C., Hermann J., Arculus R., and Mavrognes J., 2003, Redistribution of trace elements during prograde metamorphism from lawsonite blueschist to eclogite facies; implications for deep subduction-zone processes: Contributions to Mineralogy and Petrology, v. 146, p. 205-222.

Stern, R.J., 2005, Evidence from ophiolites, blueschists, and ultrahigh-pressure metamorphic terranes that the modern episode of subduction tectonics began in Neoproterozoic time: Geology, v. 33, p. 557-560.

Stern, R. J., and Bloomer, S. H., 1992, Subduction zone infancy: examples from the Eocene Izu-Bonin-Mariana and Jurassic California arcs: Geological Society of America Bulletin, v. 104, p. 1621-1636.

Stewart, M. and Fowler, A.D., 2001, The nature and occurrence of discrete zoning in plagioclase from recently erupted andesitic volcanic rocks, Montserrat: Journal of Volcanology and Geothermal Research, v. 106, p. 243-253.

Streckeisen, A.L., 1976, To each plutonic rock its proper name: Earth Science Reviews, v. 12, p. 1-33.

Streckeisen, A.L., 1979, Classification and nomenclature of volcanic rocks, lamprophyres, carbonatites, and melilitic rocks: Recommendations and suggestions of the IUGS Subcommission on the Systematics of Igneous Rocks: Geology v. 7, p. 331-335.

Sun, C.-H., and Stern, R.J. 2001, Genesis of Mariana shoshonites: contribution of the subduction component: Journal of Geophysical Research, v. 106, p. 589-608

Sun, S-S, and McDonough W.F., 1989, Chemical and isotopic systematics of oceanic basalts: implications for mantle composition and processes, *in* Saunders A.D., and Norry, M.J.,*eds*., Magmatism in the Oceanic Basins: Geological Society of London Special Publication 42, p. 313-345.

Tan, E., Gurnis, M., and Han, L., 2002, Slabs in the lower mantle and their modulation of plume formation: Geochemistry, Geophysics, Geosystems, v. 3, no. 11, 1067, doi: 10.1029/2001GC000238, 24p.

Tatsumi, Y., 2000, Slab melting, its role in continental crust formation and mantle evolution: Geophysical Research Letters, v. 27, p. 3941-3944.

Tatsumi, Y., 2005, The subduction factory, how it operates in the evolving Earth: GSA Today, v. 15, no. 7, p. 4-10.

Tatsumi, Y., and Eggins, S., 1995, Subduction Zone Magmatism: Boston, Blackwell Science, 211p.

Tatsumi, Y., and Kogiso, T., 2003, The subduction factory: its role in the evolution of Earth and Mantle, *in* Larter, R.D., and Leat, P.T., *eds*., Intra-oceanic Subduction Systems: Geological Society of London Special Publication 219, London, p. 55-80.

Taylor, S.R., 1995, The geochemical evolution of the continental crust: Reviews of Geophysics, v. 33, p. 241-265.

Thorkelson, D.J, 1996, Subduction of diverging plates and the principles of slab window formation: Tectonophysics, v. 255, p. 47-63

Thorkelson, D.J., and Breitsprecher, K., 2005, Partial melting of slab window margins: genesis of adakitic and non-adakitic magmas: Lithos, v. 79, p. 25-41.

Turner, A., Arnaud, N., Liu, J., Rogers, N.,

Hawkesworth, C., Harris, N., Kelley, S., van Calsteren, P., and Deng, W., 1996, Post-collision, shoshonitic volcanism on the Tibetan plateau: implications for convective thinning of the lithosphere and the source of Ocean Island basalts: Journal of Petrology, v. 37, p. 45-71.

Whalen, J.B., Jenner, G.A., Longstaffe, F.J., Robert, F., and Gariepy, C., 1996, Geochemical and isotopic (O, Nd, Pb and Sr) constraints on A-type granite petrogenesis based on the Topsails igneous suite, Newfoundland Appalachians: Journal of Petrology, v. 37, p. 1463-1489.

Wiebe, R.A., Blair, K.D., Hawkins, D.P., and Sabine, C.P., 2002, Mafic injections, in situ hybridization, and crystal accumulation in the Pyramid Peak granite, California. Geological Society of America Bulletin, v. 114, p. 909-920.

Wilson, M., 1989, Igneous Petrogenesis, a Global Approach. Unwin Hyman, London.

Winchester, J.A., and Floyd, P.A., 1977, Geochemical discrimination of different magma series and their differentiation products using immobile elements: Chemical Geology, v. 20, p. 325-343.

Winter, J.D., 2001, An Introduction to Igneous and Metamorphic Petrology: Prentice Hall, New Jersey, 695p.

Wood, D.A., 1979, A variably veined suboceanic upper mantle, genetic significance for mid-oceanic ridge basalts from geochemical evidence: Geology, v. 7, p. 499-503.

Wood, D.A., Joron, J.-L., and Treuil, M., 1979, A re-appraisal of the use of trace elements to classify and discriminate between magma series erupted in different tectonic settings: Earth and Planetary Science Letters, v. 45, p. 326-336.

Zhong, S., and Gurnis, M., 1997, Dynamic interaction between tectonics plates, subducting slabs, and the mantle: Earth Interactions, v. 1, p. 1-18.

Zindler, A., and Hart, S., 1986, Chemical geodynamics: Annual Review of Earth and Planetary Sciences, v. 14, p. 493-571.

APPENDIX 1: Trace Element Modelling in Igneous Rocks

For any element, the relative distribution, or **partitioning** (D) between mineral and magma, given by;

$$D = C_S/C_L$$

where C_S and C_L are the concentration of the element in the solid and liquid phases, respectively. Typical values for D (known as the **distribution coefficient** or **partition coefficient**) are shown in Table 1, (see Pearce and Norry 1979; Rollinson 1993).

As a liquid cools, more than one mineral crystallizes, and in this instance the bulk distribution coefficient, D, is used, which is the weighted average of the distribution coefficients for an element in each of the crystallizing minerals. Compatible elements have $D>>1$, whereas incompatible elements $D<<1$.

Arc magmas commonly undergo a range of processes as they cool, and three simple examples are considered here; equilibrium crystallization, fractional crystallization and magma mixing. Equilibrium crystallization (i.e. crystals remain in contact with the melt) and fractional crystallization (i.e. crystals are separated and chemically isolated from the melt) are examples of the effect of D on the trace element abundance of a cooling magma. Under equilibrium crystallization conditions, mass is conserved so that

$$C_O = C_S(1-F) + C_L(F)$$

where C_O is the starting concentration of a given element in a source, C_S is the concentration of that element in the solid and F is the fraction of magma remaining. Substituting $C_S = D.C_L$ and simplifying, we get

$$C_L/C_O = 1 / [D (1-F) + (F)]$$

(after Shaw 1970)

Curves describing the increase or decrease in elemental concentrations with the fraction of melt can be readily calculated for any element if its D is known. For example, if an element has a D = 0.1, then for F = 0.5, C_L/C_O = 1.9 and as F approaches 0, C_L/C_O approaches 10 (Fig. A1-a). The abundances of incompatible elements, therefore, increase exponentially with decreasing F (and so their abundances are often represented on log-log plots, where they commonly exhibit linear relationships, e.g. Pearce and Norry 1979). Such low percentages of melt occur in either the early stages of melting or the late stages of crystallization. The abundances of compatible elements systematically decrease with decreasing F. For example, an element with D = 10, approaches $C_L/C_O = 0.1$ as F approaches 0.

For perfect fractional crystallization of a cooling magma in a closed system (also known as Raleigh fractionation):

$$C_L/C_O = F^{(D-1)}$$

(Allègre et al. 1977)

For D = 1, $C_L = C_O = 1$. For very low D, $C_L/C_O = 1/F$, and for very high D, C_L becomes very small as F decreases.

Although they are described by different equations, equilibrium and fractional crystallization produce similar enrichment and depletion trends described by exponential curves. Simple mixing between two arc magmas (e.g. Langmuir et al. 1978), on the other hand, produces linear trends on X-Y plots (Fig. A1-b). If we mix two magmas A and B of different composition, the mixing parameter f is given by;

$$f = A/A+B$$

the concentration of elements X and Y in the mixture (M) are given by:

$X_M = X_A f + X_B(1-f)$ or $X_M = f(X_A-X_B) + X_B$ (1) and

$Y_M = Y_A f + Y_B(1-f)$ or $Y_M = f(Y_A-Y_B) + Y_B$ (2)

These equations are both in the linear form of y = mx + b. The mixing parameter, f, is the same in both equations:

$$f = (X_M - X_B)/(X_A-X_B) = (Y_M -$$

$Y_B)/(Y_A-Y_B)$
Substituting for f in (2) and simplifying gives:

$$Y_M = X_M (Y_A-Y_B)/(X_A-X_B) + (Y_BX_A - Y_AX_B)/(X_A-X_B).$$

This equation is also in a linear form (Fig. A1-b).

Magma mixing equations for elemental ratio plots have the form

$$X_M/Y_M = a/Y_M + b$$

where a and b are constants. This is the equation of a hyperbola (see derivations in Langmuir et al., 1978; Faure and Mensing, 2005). Using this equation plots such as X/Y vs 1/Y or Z/Y are linear with a slope of "a" (Fig. A1-c). However, plots such as X/Y vs Y or X/Y vs W/Z have a hyperbolic form (Fig. A1-d). The curvature of the mixing line in the latter case depends on the ratio r, where

$$r = Y_AZ_B/Y_BZ_A$$

Note that for r ~ 1, the hyperbola approximates a straight line.

The hyperbolic curves for mixing of two magmas can be readily extended to three sources by calculating the three hyperbolae that represent the combination of any two sources and interpolating between these curves (Fig. A1-e).

The above examples grossly oversimplify the range of processes that can affect trace element abundances in arc systems, but they do provide general insights into trace element behaviour during magma evolution. For further details see Allègre et al. (1978), Hanson (1978), and Langmuir et al. (1978).

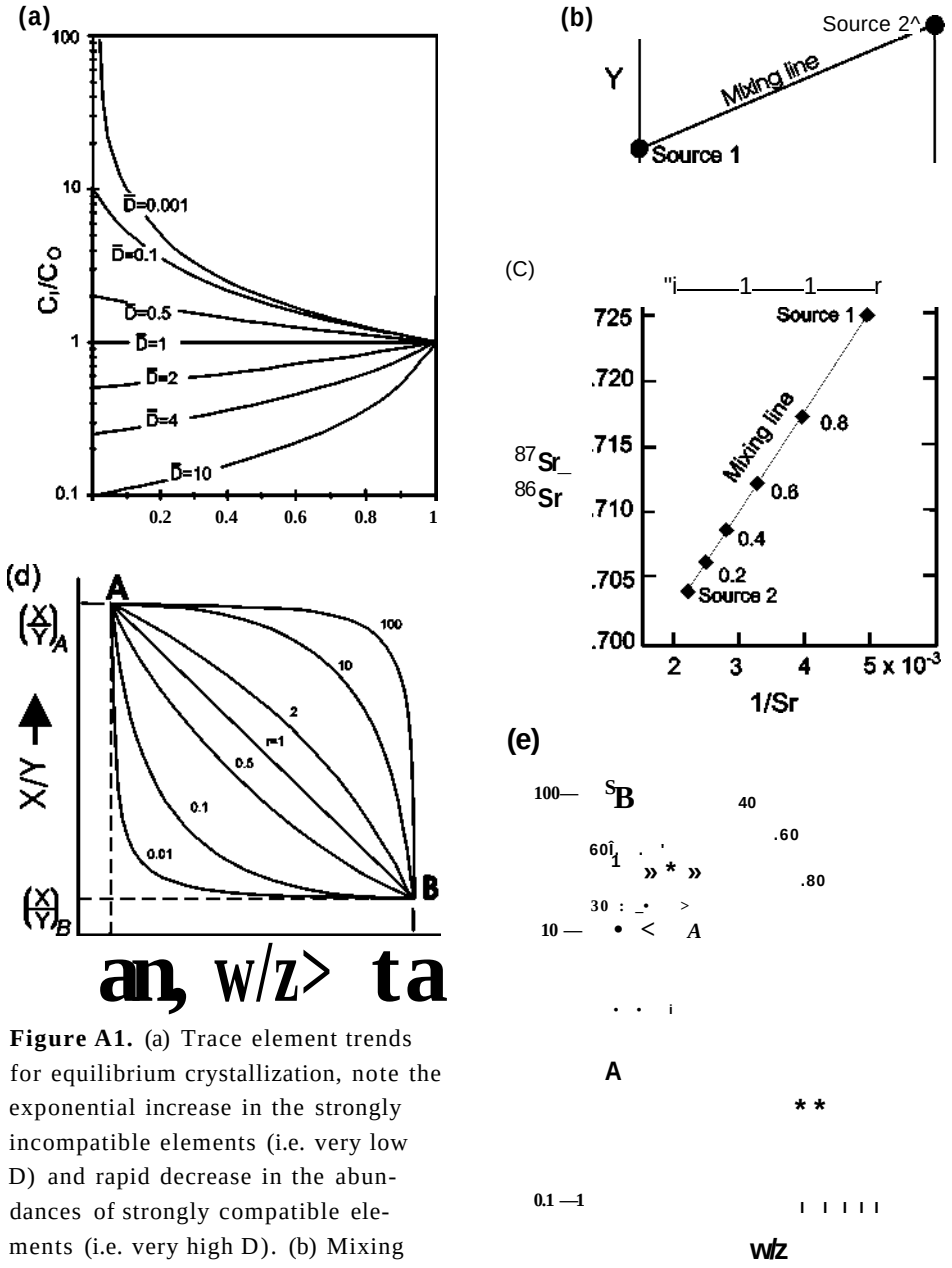

Figure A1. (a) Trace element trends for equilibrium crystallization, note the exponential increase in the strongly incompatible elements (i.e. very low D) and rapid decrease in the abundances of strongly compatible elements (i.e. very high D). (b) Mixing line in X vs Y elemental plots. (c) Ratio plots of the form X/Y vs 1/Y yield linear patterns. (d) Ratio plots of the form X/Y vs W/Z yield hyperbolic mixing lines between end members A and B for r = 0.01 to 100. (e) X/Y vs W/Z schematic diagram showing how the extent of mixing between three sources (a, b and c) can be deduced. Hyperbolic curves are drawn between two of the three sources. The area between these curves can be gridded to determine the relative contribution of each source. A hypothetical sample (filled circle) consists of 50% C, 30% B and 20% A.

Websites:

[http://www.gly.bris.ac.uk/WWW/TerraNova/arcmag/arcmag.html]

[http://serc.carleton.edu/resources/213.html]

Accepted as revised, 27 February 2007